DESIGN OF LINEAR PHASE MATCHED FILTERS WITH A CAUSAL REAL SYMMETRIC NYQUIST PULSE

BY

SALEH SANUSSI MNEINA

A Thesis
Submitted to the Faculty of Graduate Studies
In Partial Fulfillment of the Requirements for the Degree of

DOCTOR OF PHILOSOPHY

Department of Electrical and Computer Engineering
University of Manitoba
Winnipeg, Manitoba

THE UNIVERSITY OF MANITOBA

FACULTY OF GRADUATE STUDIES

*****

COPYRIGHT PERMISSION

Design of Linear Phase Matched Filters with A Causal Real Symmetric Nyquist Pulse

BY

Saleh Sanussi Mneina

A Thesis/Practicum submitted to the Faculty of Graduate Studies of The University of Manitoba in partial fulfillment of the requirement of the degree

Of

Doctor of Philosophy

I hereby declare that I am the sole author of this thesis.

I authorize the University of Manitoba to lend this thesis to other institutions or individuals for the purpose of scholarly research.

I further authorize the University of Manitoba to reproduce this thesis by photocopying or other means, in total or in part, at the request of other institutions or individuals for the purpose of scholarly research.

Saleh Sanussi Mneina

I dedicate this thesis to my mother, to my family, and to the memory of my father.

DESIGN OF LINEAR PHASE MATCHED FILTERS
WITH A CAUSAL REAL SYMMETRIC NYQUIST PULSE

Saleh Sanussi Mneina

Abstract

Real symmetric pulse transmission under a linear phase condition is formally presented. The delayed raised-cosine pulse is considered, and a novel design method used to generate a Nyquist pulse with a linear phase polynomial for the denominator of the transfer function and an appropriate placing of the zeros of the numerator is described. The combination of even symmetry of the time response, and $j\omega$-axis transmission zero pairs leads to a linear phase pulse shaping filter which is its own match. Various aspects of the linear phase design method are investigated, using least-mean-square (LMS) timing error and the jitter performance of the pulse as figures of merit. A pulse symmetry factor is also defined and used. The maximum number of finite transmission zero pairs which guarantees zero pulse amplitude at $t = 0$ is derived, and the generated pulse has negligible energy outside the main lobe and better jitter performance than the standard raised-cosine spectrum pulse. The design method is flexible, and computationally robust. The transmission zero pairs on the $j\omega$-axis enable filter implementation in terms of ladder LC networks, with high stop-band attenuation and low component sensitivity. The causal real symmetric pulse method is extended to the discrete time domain and the discrete-time raised-cosine pulse. The transmission zeros of the discrete-time raised-cosine pulse are finite. Consequently the transfer function of the shaping filter is no longer an approximation, but is exactly obtained from the z-transform of the pulse, and the discrete-time raised-cosine is perfectly reconstructed as the unit-sample response of the filter. FIR filters for various values of the delay parameter are described.

Acknowledgements

I am very grateful to my supervisor, Professor Gert Martens, for his valuable advice and guidance throughout the course of this work. His expert help and genuine kindness are profoundly appreciated. I am also grateful to Professor Edward Shwedyk of the Electrical and the Computer Engineering Department and Professor Henry Finlayson of the Department of Mathematics for a thorough review and many useful suggestions.

I would like to thank Mr. Guy Jonatschick, the ECE Unix Network administrator for the excellent computing resources which he made available, and Mr. Jeffrey Anderson, the Internet Innovation Centre Executive Director, for use of the facility.

I would also like to thank all members of the staff of the Electrical and the Computer Engineering Department and the staff of the Engineering Library at the University of Manitoba for their kindness and friendship during the course of my studies.

Finally, I would like to acknowledge the financial support of the Libyan Ministry for Higher Education which enabled me to begin this study.

Contents

List of Figures

List of Tables

Chapter 1

Introduction

1.1 Background

Nyquist's First Criterion for distortionless transmission of a data signaling waveform is that the contribution from other signaling elements must be zero at the mid point of the signaling interval, otherwise distortion results and is termed intersymbol interference (ISI). In particular, a pulse with time axis crossings is said to be a Nyquist I pulse if it satisfies the Nyquist first criterion which implies equally spaced crossings of the time axis. This criterion first appeared in [1], where the theoretical foundation for transmission of telegraph signals over a bandlimited cable with zero ISI were presented by Nyquist. Nyquist stipulated the following two axioms:

1) The time is divided into equal signaling intervals.

2) There is a finite number of conditions and each signaling interval is characterized by a single one of these conditions.

The pulse with a square spectrum was derived as the minimum bandwidth ISI free pulse, but having a tail with a slow rate of decay of $1/t$ rendered it practically useless. In fact, any real shape factor having odd symmetry about the bandedge of the frequency spectrum can be added to the frequency spectrum of this pulse thereby expanding the bandwidth and

still maintain ISI free transmission. Further research investigating pulse spectrum rolloffs that can be used for Nyquist pulse design with less severe timing error sensitivity followed thereafter, leading at some point to establishing the pulse with the raised-cosine rolloff spectrum as the standard pulse for ISI free transmission.
An introduction to Nyquist's paper can be found in [2].

The Nyquist's Second Criterion is that the interval between the instants when the received pulse passes through the mean value, shall be the same as the corresponding interval at the transmitting end. For distortionless transmission, the pulse is sampled at the end of the sampling period so that the response is due in part to the current signaling element and in part to the next signalling element. Hence the name partial response signalling. ISI is partially introduced in this case, yet the signal is recoverable since the ISI is controlled. A pulse with a cosine spectrum is derived as the pulse satisfying Nyquist's Second Criterion. In addition, any real shape factor having even symmetry about the band-edge of the frequency spectrum can be added to the frequency spectrum of this pulse and still satisfy the criterion.

Nyquist's Third Criterion pertains to preservation of pulse area, i.e., during any signalling interval, the area of the received pulse is equal to the area of the transmitted pulse. This criterion is useful for some systems used for picture transmission for which a minimum bandwidth frequency shape factor that satisfy the third criterion is also derived.

Extensive research has been undertaken to select the best approach to design the pulse shaping network or filter, this work is concerned with pulse shaping for data transmission without ISI, and will be focused on the Nyquist I pulse design, which will hereafter be referred to simply as the Nyquist pulse. Due to the large number of research publications in the area, one reference will be given as an example of each of the following approaches.

An attempt to relax the bandwidth restriction thereby extending the Nyquist first criterion to more pulse shapes can be found in [3]. Some researchers attempt to satisfy frequency domain and time domain requirements simultaneously [4], while others are restricted to the time domain [5]. Both approaches lead to a nonlinear system of equations. A third approach attempts to derive the filter directly in the frequency domain with conditions on amplitude, and phase simultaneously imposed [6], the resulting equations are linear but because the polynomial representing the numerator and the denominator of the filter transfer function are in coefficient form, the results are vulnerable to computational inaccuracies as the filter order increases. A family of nonlinear phase pulse shaping filters which is ISI free with or without matched filtering is proposed in [7]. Another [8] uses results in [3] and phase compensation to generalize the raised-cosine spectrum pulse and design a square root Nyquist filter. A worst-case design criterion is used in [9] to develop closed-form time-domain expressions for generating a Nyquist pulse which is superior to the raised-cosine spectrum pulse in terms of sensitivity to timing error. Unrealizable spectrum shape is used as a target for filter design to minimize the pulse's least-mean-square (LMS) timing, phase, or mixed error [10].These are useful in terms of providing an analytic expression for the pulse and the error, which can be used to compare different pulses.

1.2 Research Motivation and Objective

In the context of pulse transmission through a bandlimited channel corrupted with additive white Gaussian noise (AWGN), the pulse generated by the shaping filter at the transmitter, and transmitted through the channel, is required to be matched to the receive filter in order to maximize the output signal-to-noise ratio. The output of the receive filter is the received pulse. An interesting relation exists between the pulse symmetry and the phase characteristic which, along with its possible implication on the matched filter design, requires formal investigation. Furthermore, the received pulse is sampled at integer multiples of the sampling period T. Timing jitter can be caused by variations of the pulse positions or sampling instants, consequently the actual sampling instants do not occur at exact multiples of T producing a sampling error.

The objective of this research is as follows:

1) To design a Nyquist pulse that performs better in the presence of timing jitter than the raised-cosine spectrum pulse. The received pulse duration is ideally required to be limited to the interval $[0, T]$ where T is the sampling period at the receiver. Furthermore the pulse must have a negligibly small amplitude at and near the points $t = 0$ and $t = T$. A causal real pulse which has even symmetry, such as the time-domain raised-cosine pulse, satisfies these two conditions.

2) To investigate the relation between pulse symmetry and the phase characteristic and use it to design a transmit and receive matched filter pair.

It is also part of the objective that the design method should be free of the computational problems and complications of some of the methods reviewed above.

1.3 Overview

This thesis is organized as follows. Chapter **2** reviews and elaborates on the worst-case and the LMS design criterion. Closed form expressions are derived for the Nyquist pulse using both criteria. The error performance –versus excess bandwidth– for each pulse is compared with the other and with that of the raised-cosine spectrum pulse.
The triangular spectrum generated in Chapter **2** under the worst-case design criterion is used as a target for filter design in Chapter **3**, where actual pulse performance in the presence of jitter is compared to that of the raised-cosine spectrum pulse.

In Chapter **4**, the relationship between the causal real symmetric pulse and the linear phase characteristic is formally proved; it is shown that linear phase is a necessary and sufficient condition for symmetric impulse response. The delayed time-domain raised-cosine pulse is considered for the output of the shaping filter at the transmitter, whose transfer function is approximated by a linear phase denominator polynomial, and transmission zero pairs which are placed on the $j\omega$-axis in accordance with the attenuation response of the time-domain raised-cosine pulse. The generated pulse is essentially contained within the main lobe as required. The combination of even symmetry of time response, and conjugate transmission zero pairs leads to a linear phase pulse shaping filter which is its own match. A matched transmit and receive filter pair is presented, and the overall minimum stopband attenuation is 66 dB. Performance of the receive pulse in the presence of jitter is quite satisfactory, and the sampling error is virtually zero.

The linear phase design is investigated further in Chapter **5**, where numerous design examples of linear phase filters of various orders are discussed. Performance of the causal real symmetric pulse is evaluated by comparison to the raised-cosine pulse using design figures of merits which were derived in previous chapters; a factor quantifying pulse symmetry is also introduced and used. A transfer function realization as a ladder LC network is given. An algorithm for placing the zeros of the numerator to produce an attenuation response of arbitrary shape is described and a filter design example is given.

The causal real symmetric pulse treatment presented in Chapter **4** in the continuous time domain, is extended to the discrete time domain in Chapter **6**.

The frequency response of the discrete-time delayed raised-cosine pulse is derived with the delay as a parameter. Unlike the continuous-time raised-cosine pulse, its attenuation response has a finite number of transmission zero pairs. The z-transform of the delayed raised-cosine pulse is also derived leading to an FIR filter design, which exactly produces the raised cosine pulse. Filter transfer function examples are given for various orders and delay values, and a filter realization example is given.

Finally, Chapter **7** states the conclusions.

Chapter 2

Timing Error Analysis and The Nyquist Pulse Design

For transmission through a band-limited channel without intersymbol interference, the time response must satisfy the Nyquist Criterion. A particular pulse that has been widely used in practice corresponds to the raised-cosine rolloff spectrum with bandwidth which exceeds half the symbol rate. It is called the raised-cosine pulse. However, this pulse is not unique.

Methods for generating different pulse shapes which satisfy the Nyquist Criterion are discussed. Two methods from the literature are reviewed and elaborated on. The first method is based on a worst-case design criterion and produces a pulse with triangular rolloff spectrum. The second method is based on a least-mean-square error criterion to analyse pulse sensitivity to timing errors. It leads to an optimum pulse. Each pulse is superior to the raised-cosine pulse in terms of sensitivity to timing errors under the corresponding criterion. Closed form expressions are derived for the Nyquist pulse using both methods, and the error performance –versus excess bandwidth– for each pulse is compared with the other and with that of the raised-cosine pulse.

2.1 Introduction

For transmission through a band-limited channel without intersymbol interference (ISI), the time response $p(t)$ must satisfy the Nyquist criterion; a pulse satisfying this criterion is called a Nyquist pulse. The Nyquist pulse is not unique as numerous band-limited functions satisfying the Nyquist criterion can be found, in particular, the pulse with the raised-cosine rolloff spectrum, is widely used. This is the raised-cosine rolloff pulse which is known as the standard raised-cosine pulse. It will be referred to as the raised-cosine spectrum pulse, and should not be confused with the raised-cosine in the time domain pulse which will be discussed in Chapter 4.

In this chapter pulses other than the raised-cosine spectrum pulse whose Fourier transforms are band-limited and satisfy the Nyquist criterion for a given repetition rate are investigated. The following section reviews the Nyquist criterion and the Nyquist pulse. Use of the worst-case design criterion to generate Nyquist pulses was reported in [9] in abbreviated form. This design criterion is elaborated on in greater detail in Sect. **2.3.1**. where the Nyquist pulse is generated in closed-form time-domain expressions.
The timing sensitivity corresponding to the worst-case design is developed in greater detail in Sect. **2.3.2**, where worst-case design error curves for the raised-cosine spectrum pulse and the resulting pulse versus the rolloff factor are also generated. The latter pulse exhibits a smaller worst-case error for all values of the rolloff factor α [11].

Sect. **2.4** reviews, and presents a detailed treatment of, the least-mean-square method to analyze pulse sensitivity to the timing error and development of an optimum pulse [10]. For comparison least-mean-square design error curves have also been generated for the

optimum pulse, the triangular and the raised-cosine spectrum pulse.

The conclusions are presented in Sect. **2.5**.

2.2 The Nyquist Pulse

For transmission through a band-limited channel without intersymbol interference (ISI), the time response $p(t)$ must satisfy the Nyquist criterion:

$$p(nT) = \begin{cases} 1 & n = 0 \\ 0 & n \neq 0 \end{cases} \qquad n \in I \tag{2-1}$$

where T is the sampling period. In the frequency domain, the above condition corresponds to [12]

$$\sum_{k=-\infty}^{\infty} P(f - k/T) = P(0) \tag{2-2}$$

where $P(f)$ is the Fourier transform of $p(t)$.

When the time response $p(t)$ represents the impulse response, the Fourier transform $P(f)$ is known as the Nyquist filter and may represent the over all system response incorporating the transmit filter, the channel, and the receive filter.

If the channel is band-limited to some frequency B, then consequently, the spectrum of the baseband pulse $p(t)$, $P(f) = 0 \ \ for \ \ |f| > B$.

When $B = 1/2T$, the available bandwidth equals half the symbol rate, then (2-2) is clearly satisfied by the unique pulse $p(t) = \dfrac{\sin(\pi t/T)}{\pi t/T}$ with a square spectrum but the corresponding filter is unrealizable. Even a close approximation to the pulse $\dfrac{\sin(\pi t/T)}{\pi t/T}$

would require a complicated filter to approximate the abrupt transition band, and more importantly, the performance is very sensitive to timing errors due to the slow rate of decay of the tail of the pulse.

Assume a small timing error Δ in sampling the signal $p(t) = \frac{\sin(\pi t/T)}{\pi t/T}$. Then for the case of binary data of ± 1 the ISI contribution in a worst-case scenario is

$$\sum_{\substack{n=-\infty \\ n\neq 0}}^{\infty} |p(nT+\Delta)| = \sum_{\substack{n=-\infty \\ n\neq 0}}^{\infty} \frac{|\sin(\pi(\Delta/T))|}{|\pi(n+\Delta/T)|} = \begin{cases} 0 & for\ \Delta = 0 \\ \infty & for\ \Delta \neq 0 \end{cases}$$

The worst-case ISI is infinite for any nonzero timing error and a sampling error is devastating in this case primarily because $p(t)$ decays only as $1/t$.

For a receive filter that eliminates ISI to be realized, it is necessary that the bandwidth B exceeds half the symbol rate $1/2T$, where T is the sampling period and $f_s = 1/T$ is the sampling frequency. Moreover, to simplify filter design and improve performance sensitivity to timing errors, the bandwidth must approach $1/T$.

The amount of bandwidth in excess of the Nyquist band $1/2T$ is referred to as the excess bandwidth, and the relative excess bandwidth is called the rolloff factor $\alpha = \frac{B - 1/2T}{1/2T}$.

When $1/2T < B < 1/T$ (note that then $0 < \alpha < 1$), the Nyquist criterion (2-2) is equivalent to requiring that $P(f)$ have a symmetry point at $f = f_s/2 = 1/2T$

$$P\left(\frac{1}{2T}+f\right) + P^*\left(\frac{1}{2T}-f\right) = P(0) \qquad for\ |f| < \frac{1}{2T} \tag{2-3}$$

The Nyquist pulse is not unique in this case and numerous functions with $1/2T < B < 1/T$ and satisfying the above symmetry can be found; a particular spectrum

that satisfies the above condition and has been widely used in practice is the raised-cosine rolloff spectrum

$$P(f) = \begin{cases} 1 & |f| \le f_1 \\ \frac{1}{2}\left\{1 - \sin\left[\frac{\pi T}{\alpha}\left(|f| - \frac{1}{2T}\right)\right]\right\} & f_1 \le |f| \le f_2 \\ 0 & |f| > f_2 \end{cases} \tag{2-4}$$

where $f_1 = (1-\alpha)/2T$, $f_2 = (1+\alpha)/2T$, and α is the rolloff factor, $0 \le \alpha \le 1$.

The corresponding pulse, termed the raised-cosine spectrum pulse, is given by

$$p(t) = \frac{\sin(\pi t/T)}{\pi t}\frac{\cos(\alpha\pi t/T)}{1-(2\alpha t/T)^2} \tag{2-5}$$

The raised-cosine spectrum pulse crosses the time axis at the sampling instants, and has sidelobes that decrease with increasing rolloff factor α, from 0 to 1 as shown in Fig. 2.1. The rate of decay is $1/t^3$ and is a substantial improvement over the square pulse and timing errors are not as devastating.

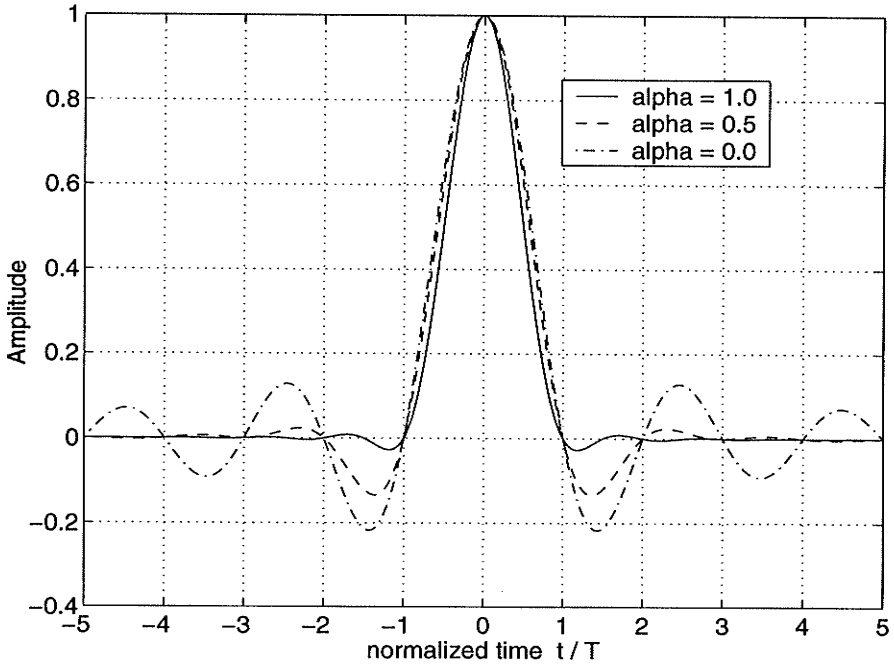

Fig. 2.1 The raised-cosine spectrum pulse for different values of the rolloff factor

2.3.1 The Worst-Case Design Method

The spectrum of the pulse, $P(f)$ is assumed to be real, even, and odd about $f_s/2$ in the range $f_1 \le f \le f_2$, $f_s/2 = 1/2T$ is the symmetry point mentioned in relation to (2-3) above, and $P(0) = 1$. Define $G(f) = 2P(f) - 1$, a scaled and amplitude shifted version of $P(f)$ (see Fig. 2.2), then $G(f)$ is also even. Then from (2-3)

$$P(f) + P(f_s - f) = 1 \Leftrightarrow G(f) + G(f_s - f) = 0$$

Thus this latter condition is necessary and sufficient for the pulse to be a Nyquist pulse.

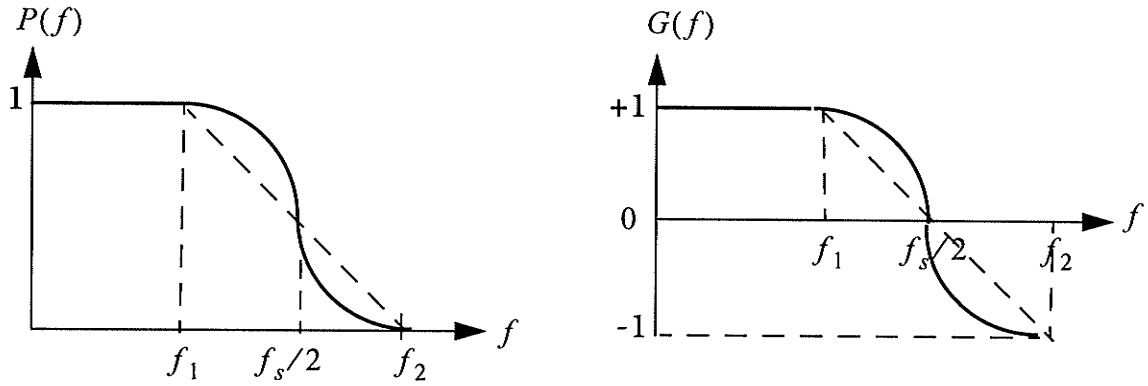

Fig. 2.2 The raised-cosine and the triangular functions

The Nyquist pulse is generated in a closed form expression [9]

$$p(t) = \frac{1}{\pi t}\sin(\pi f_s t) \int_0^{\alpha f_s/2} \phi(f)\cos(2\pi f t)df = \frac{1}{\pi t}\sin(\pi f_s t)\ g(t) \qquad (2\text{-}6)$$

$$g(t) = \int_0^{\alpha f_s/2} \phi(f)\cos(2\pi f t)df \qquad (2\text{-}7)$$

$g(t)$ is then the inverse transform of $\phi(f)/2$, and $\phi(f)$ is an arbitrary real even function of f which is band-limited to $\pm\alpha f_s/2$ such that $\int_0^{\alpha f_s/2} \phi(f)df = 1$, and $p(t)$ is

a solution to (2-1). $P(f)$ is therefore the convolution of $\phi(f)/2$ and a rectangular function which is band-limited to $\pm f_s/2$. Eq. (2-6) is a closed-form time-domain expression for generating pulses satisfying the Nyquist criterion, (see Appendix **A1**).

For example, consider the raised-cosine spectrum pulse given in (2-5) as a special case of a pulse satisfying (2-1). From (2-6) we deduce that the corresponding function $g(t)$ is given by $g(t) = \dfrac{\cos(\alpha\pi f_s t)}{1-(2\alpha f_s t)^2}$. To obtain the corresponding function $\phi(f)$ a new function $Q(f)$ is defined as a shifted version of $G(f)$ according to the relation

$$Q(f) = G(f + f_s/2) = -\sin\left(\frac{\pi}{\alpha}\frac{f}{f_s}\right) \quad for \ -\alpha f_s/2 \le |f| \le \alpha f_s/2$$

where $G(f)$ is obtained from the spectrum (2-4) as

$$G(f) = 2P(f) - 1 = -\sin\left(\frac{\pi}{\alpha f_s}(f - f_s/2)\right) \ for \ f > 0;$$

It follows that (see Appendix **A1**) $\phi(f) = -\dfrac{d}{df}Q(f) = \dfrac{\pi}{\alpha f_s}\cos\dfrac{\pi f}{\alpha f_s}$.

A triangular $G(f)$ was proposed as

$$G(f) = \frac{f_s/2 - |f|}{\alpha f_s/2} \quad for \ (1-\alpha)f_s/2 \le |f| \le (1+\alpha)f_s/2 \tag{2-8}$$

The spectrum of the pulse in this case is given by

$$P(f) = \begin{cases} 1 & |f| \le (1-\alpha)f_s/2 \\ \dfrac{1}{2} + \dfrac{f_s/2 - |f|}{\alpha f_s} & (1-\alpha)f_s/2 \le |f| \le (1+\alpha)f_s/2 \\ 0 & |f| > (1+\alpha)f_s/2 \end{cases} \tag{2-9}$$

$P(f)$ is an even function of f and $G(f)$ has odd symmetry about $f = f_s/2$, and (2-2) is clearly satisfied. This particular case is named the triangular function after the triangular rolloff of the spectrum.

Similar to the raised-cosine rolloff case, to derive the pulse corresponding to the triangular rolloff define $Q(f) = G(f + f_s/2) = -\frac{2f}{\alpha f_s}$ $\quad for\ -\alpha f_s/2 \le |f| \le \alpha f_s/2$

substituting $\phi(f) = -\frac{d}{df}Q(f) = \frac{2}{\alpha f_s}$ into (2-7) and integrating to get

$$g(t) = \frac{\sin(\pi\alpha f_s t)}{\pi\alpha f_s t} = Sa(\pi\alpha f_s t) \tag{2-10}$$

where Sa is the sampling function defined as $Sa(x) = \sin x/x$, from (2-6)

$$\begin{aligned} p(t) &= \frac{\sin(\pi f_s t)}{\pi t} g(t) = \frac{\sin(\pi f_s t)}{\pi t}\frac{\sin(\pi\alpha f_s t)}{\pi\alpha f_s t} \\ &= f_s Sa(\pi f_s t) Sa(\pi\alpha f_s t) \end{aligned} \tag{2-11}$$

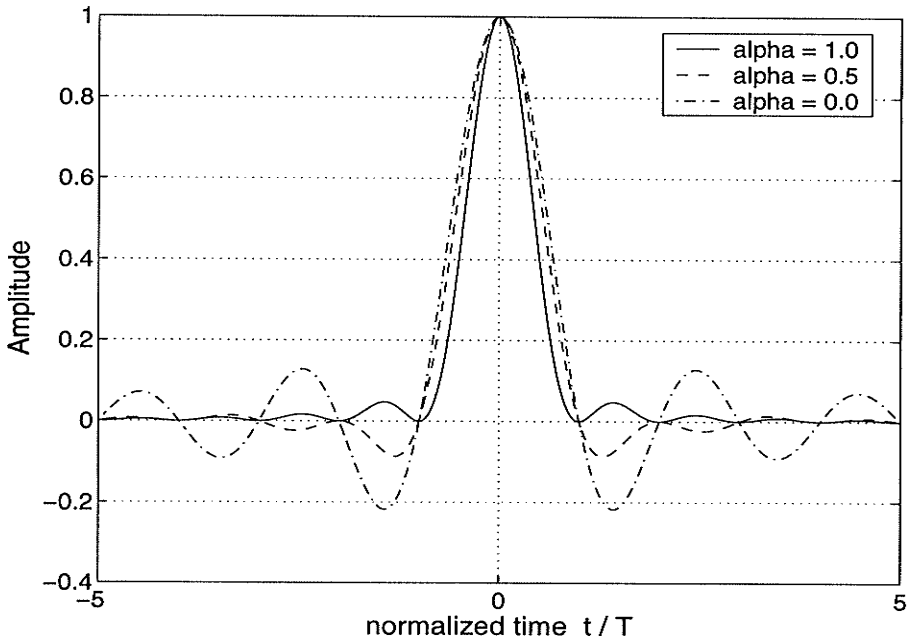

Fig. 2.3 The triangular pulse for different values of the rolloff factor

2.3.2 Timing Error for the Worst-Case Design

A worst-case design criterion is adopted to analyse pulse sensitivity to timing error [9]. Assuming a small timing error Δ, and a received pulse represented by the pulse train $\sum_{n=-\infty}^{\infty} a_n p(t-nT)$ the interfering signal for detection at $t = 0$ is $\sum_{\substack{n=-\infty \\ n\neq 0}}^{\infty} a_n p(t-nT)$

The ISI is to a first order approximation $\Delta \sum_{\substack{n=-\infty \\ n\neq 0}}^{\infty} \left| a_n \frac{d}{dt} p(t-nT) \right|$ evaluated at $t = 0$.

At $t = 0$ the term under consideration has amplitude a_o, it is the term which is being interfered with by all other terms, and we have (see Appendix **A2**)

$$ISI = \frac{\Delta}{T} \sum_{\substack{n=-\infty \\ n\neq 0}}^{\infty} (-1)^{n+1} \ (a_n/a_o) \frac{g(nT)}{n} \tag{2-12}$$

In binary transmission $a_n = \pm 1$, for a worst-case situation the a_n are chosen such that all interfering terms add. Then the worst-case for the appropriate choice of the a_n gives

$$ISI = \frac{2\Delta}{T} \sum_{n=1}^{\infty} \frac{|g(nT)|}{n} \tag{2-13}$$

Substituting the function $g(nT) = \frac{\sin(\alpha n\pi)}{\alpha n\pi} = Sa(\alpha n\pi)$, which corresponds to the triangular rolloff spectrum into (2-13), we get an upper bound for the worst-case sensitivity of the triangular function:

$$ISI|_{Triangular} = \frac{2\Delta}{T} \sum_{n=1}^{\infty} \left| \frac{\sin(\alpha n\pi)}{\alpha n^2 \pi} \right| \leq \frac{2\Delta}{\alpha\pi T} \sum_{n=1}^{\infty} \frac{1}{n^2} = \frac{2\Delta}{\alpha\pi T} \frac{\pi^2}{6} = \frac{\pi}{3\alpha} \frac{\Delta}{T} \tag{2-14}$$

For the special case when $\alpha = 1/2$ we get

$$ISI|_{Triangular} = \frac{4\Delta}{\pi T}\sum_{n=1}^{\infty}\left|\frac{\sin(n\pi/2)}{n^2}\right| = \frac{4\Delta}{\pi T}\sum_{m=1}^{\infty}\frac{1}{(2m-1)^2} = \frac{4\Delta}{\pi T}\frac{\pi^2}{8} = \frac{\pi\Delta}{2T} = 1.5708\frac{\Delta}{T} \tag{2-15}$$

where $\sin(n\pi/2) = 0$ *for* n *even* has been used.

The worst-case error for the triangular pulse is shown in Fig. 2.4, versus the relative excess bandwidth (the rolloff factor α), which assumes values between 0 and 1.

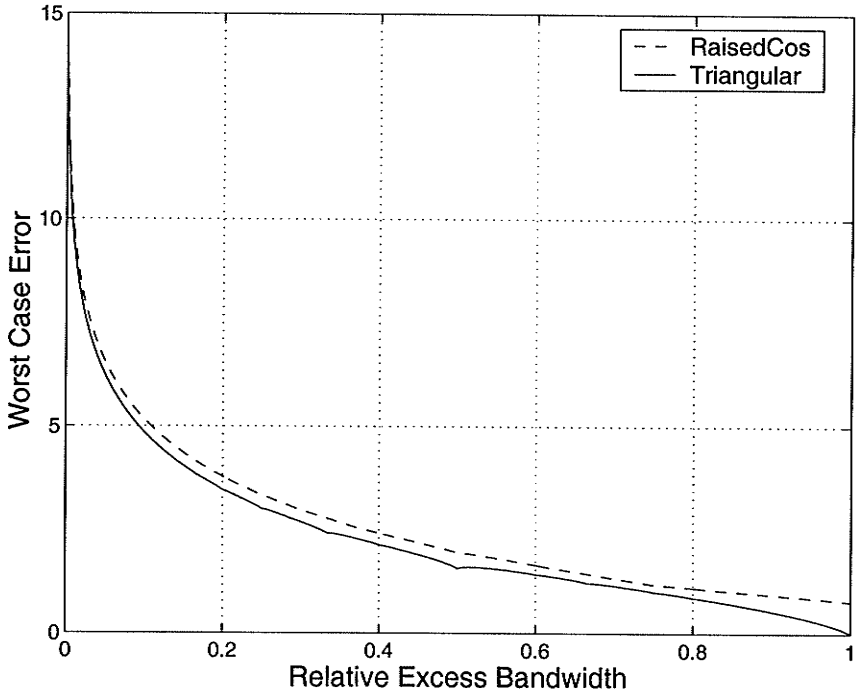

Fig. 2.4 Comparison of worst-case errors

Similarly, substituting the function $g(nT) = \dfrac{\cos(\alpha n\pi)}{1-(2\alpha n)^2}$ corresponding to the raised-cosine rolloff spectrum into (2-13), we get an expression for worst-case sensitivity for the the raised-cosine spectrum pulse

$$ISI|_{raised\,cosine} = \frac{2\Delta}{T}\sum_{n=1}^{\infty}\left|\frac{\cos(\alpha n\pi)}{n(1-4\alpha^2 n^2)}\right| \tag{2-16}$$

which can be computed for given values of the timing error Δ and the rolloff factor α.

For $\alpha = 1/2$, (2-16) becomes

$$ISI|_{raised\,cosine} = \frac{2\Delta}{T}\sum_{n=1}^{\infty}\left|\frac{\cos(n\pi/2)}{n(1-n^2)}\right| = \frac{\Delta}{T}\left\{\frac{\pi}{2} + \sum_{n=1}^{\infty}\frac{1}{n(4n^2-1)}\right\}$$

In the above sum n has been replaced by $2n$ because except for $n = 1$ odd values do not contribute. Since $\sum_{n=1}^{\infty}\dfrac{1}{n(4n^2-1)} = 2\ln 2 - 1$ [13], and by L'hospital's rule we have

$$\left.\frac{\cos(n\pi/2)}{n(n^2-1)}\right|_{n=1} = \left.\frac{-\frac{\pi}{2}\sin(n\pi/2)}{3n^2-1}\right|_{n=1} = -\frac{\pi}{4}, \text{ then follows}$$

$$ISI|_{raised\,cosine} = \frac{\Delta}{T}\left\{\frac{\pi}{2} + 2\ln 2 - 1\right\} = 1.957\frac{\Delta}{T} \tag{2-17}$$

This is the expression for the worst-case sensitivity corresponding to the raised-cosine rolloff for $\alpha = 1/2$.

The worst-case error for the raised-cosine spectrum pulse is also shown in Fig. 2.4.

2.4 Timing Error and Least-Mean-Square Design

A least-mean-square (LMS) error criterion can be used to analyse pulse sensitivity to timing errors and obtain an optimum pulse [10]. The mean squared error in the received signal sample has a parabolic behaviour near the origin.

The Fourier Transform of the pulse chosen to minimize the error near the origin should satisfy the Nyquist criterion stated in (2-2), that is $\sum_{n=-\infty}^{\infty} P(f-n/T) = P(0) = T$.
It is convenient to write $P(f)$ in terms of a rolloff function $B(f)$:

$$P(f) = T[P_0(f) + B(f-1/2T) + B^*(-f-1/2T)] \tag{2-18}$$

where $B(f) = 0$ for $|f| > \alpha/2T$ and

$$P_0(f) = \begin{cases} T & |f| < 1/2T \\ 0 & otherwise \end{cases} \tag{2-19}$$

Note that $P(f)$ reduces to $P_0(f)$ when $\alpha = 0$.

The Nyquist constraint (2-2) is equivalent to $B(f) = -B^*(-f)$, which implies that $ImB(f)$ is even. Franks [10] derived the following expression for the mean squared timing error:

$$LMS\ E_t = \left(\frac{2\pi}{T}\right)^2\left[\frac{1}{6} - 4T\int_0^{\alpha/2T} B(f)[1-B(f)]df + 8T^2\int_0^{\alpha/2T} fB(f)df\right]. \tag{2-20}$$

Minimization of the timing error by use of the calculus of variations [14] (see Appendix **A3**), leads to an optimum rolloff function

$$B(f) = \frac{1}{2} - Tf, \quad 0 \le f \le \alpha/2T \tag{2-21}$$

Substituting this rolloff function in (2-20) produces the LMS timing error

$$LMS\ E_t = \left(\frac{2\pi}{T}\right)^2\frac{1}{6}(1-\alpha)^3 \tag{2-22}$$

which corresponds to the LMS timing error optimum pulse

$$p(t) = S_a(\pi t/T)((1-\alpha)\cos(\alpha\pi t/T) + \alpha S_a(\alpha\pi t/T)) \tag{2-23}$$

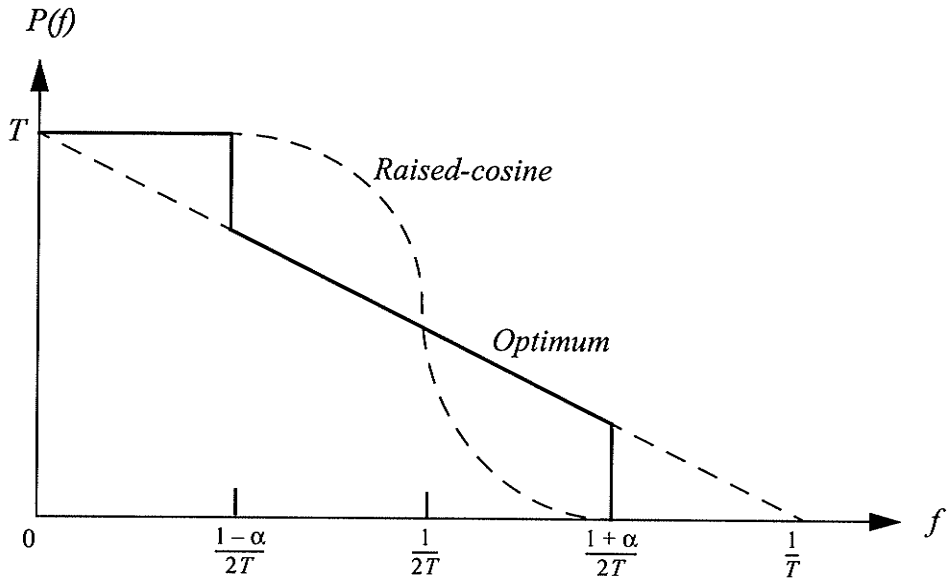

Fig. 2.5 Spectrum of the Optimum pulse and the raised-cosine pulse

The Fourier Transform of the timing error optimum pulse is shown in Fig. 2.5 (solid line); the raised-cosine rolloff spectrum is also shown (dotted line). Note that the value at zero frequency is T not unity as for the worst-case design (see Fig. 2.2).

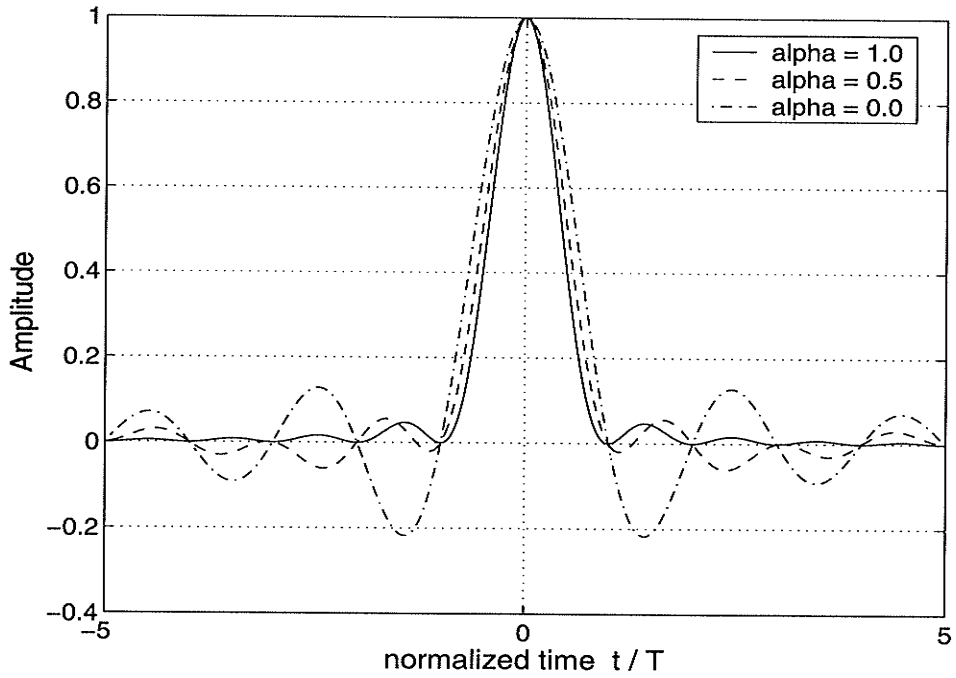

Fig. 2.6 The optimum pulse for different values of the rolloff factor

The spectrum of the optimum pulse is discontinuous and the optimum pulse is not contained within the main lobe as shown in Fig 2.6. Note that the timing error optimum pulse is the same as the triangular pulse of Sect. **2.3.1** for rolloff values 0, and 1.

The corresponding expressions for the raised-cosine spectrum pulse are

$$B(f) = \frac{1}{2}\left(1 - \sin\frac{\pi T f}{\alpha}\right), \quad 0 \le f \le \alpha/2T \tag{2-24}$$

$$LMS \;\; E_t = \left(\frac{2\pi}{T}\right)^2 \frac{1}{6}\left[1 - \frac{3}{2}\alpha + 3\left(1 - \frac{8}{\pi^2}\right)\alpha^2\right] \tag{2-25}$$

Performance of the triangular pulse (obtained under worst-case design consideration), can also be determined under the LMS conditions. The corresponding expressions are

$$B(f) = \frac{1}{2}\left(1 - \frac{f}{\alpha/2T}\right), \quad 0 \le f \le \alpha/2T \tag{2-26}$$

$$LMS\ E_t = \left(\frac{2\pi}{T}\right)^2 \frac{1}{6}(1-\alpha)^2 \tag{2-27}$$

The LMS timing error curves of the optimum pulse (2-23), the raised-cosine spectrum pulse (2-25), and the triangular pulse (2-27) are shown in Fig. 2.7 versus the rolloff factor α. Since the triangular pulse is optimum for values of $\alpha = 0$, and 1, the LMS errors are equal for the optimum pulse and the triangular pulse at the end points where the two pulses are the same.

Conversely, performance of the pulse obtained under the LMS consideration cannot be determined under the worst-case design conditions of the previous section.

To obtain the ISI in this case the function $g(nT) = \alpha Sa(\alpha n\pi) + (1-\alpha)\cos(\alpha n\pi)$, is to be substituted into (2-13), and due to the presence of periodic functions in the expression of g, the infinite series $\sum_{n=1}^{\infty} \frac{|g(nT)|}{n}$ does not converge.

The ISI cannot be determined for this case. However we expect the optimum pulse to have the same ISI at $\alpha = 0, 1$ as the triangular pulse since the two pulses are the same there. The triangular pulse has better performance than the raised-cosine spectrum pulse under the worst-case design criterion, as well as under the LMS design.

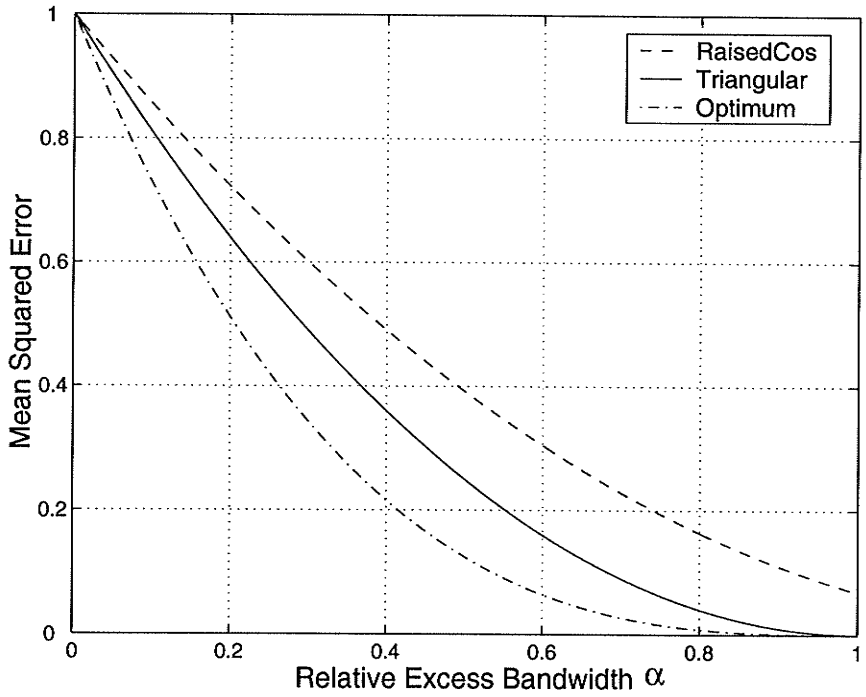

Fig. 2.7 Comparison of mean squared timing errors

2.5 Conclusions

The Nyquist pulse is generated from closed-form time-domain expressions which are developed in greater detail in this chapter than is found in the literature. Development of the triangular pulse has been carried out further than was reported in the literature, and worst-case design error curves for the triangular pulse and the raised-cosine spectrum pulse versus the rolloff factor are generated. Detailed treatment of Franks' analysis of the timing error and development of an optimum pulse has been presented, and LMS design error curves have been generated; these curves indicate superiority of the optimum pulse over the raised-cosine spectrum pulse.

The triangular rolloff spectrum which corresponds to the worst-case design is a continuous function of frequency as can be seen from Fig. 2.2, while the spectrum corresponding to the LMS Design Method is discontinuous (Fig. 2.5), therefore, there is no curve corresponding to the optimum pulse (in the LMS sense) in Fig. 2.4. The series representing the ISI (2-13) is shown to be divergent when computed for the optimum pulse under the worst-case design condition. The triangular pulse has better performance than the raised-cosine spectrum pulse under the worst-case design criterion, as well as under the LMS design.

Both spectra used in conjunction with the worst-case and the least-mean-square method imply an infinite attenuation for the entire stopband which can not be achieved with practical filters. Hence, the triangular rolloff spectrum and the spectrum corresponding to the optimum pulse are theoretical results that cannot be exactly produced in practice as practical filters do not have infinite attenuation over the entire stopband. The filter necessarily cannot be strictly bandlimited.

Chapter 3

The Triangular Pulse and Linear Phase Filter Design

Filter design for data transmission involves the search for functions with certain properties, which when used as targets, the resulting filter will be appropriate for a predetermined task, such as, reduction of jitter effect. A widely used class of baseband pulses that satisfy the Nyquist Criterion for eliminating intersymbol interference (ISI) in narrowband communications are pulses with zero crossings at the sampling instants corresponding to the standard raised-cosine spectrum. In this chapter, use of an alternative pulse, one with zero derivatives at the sampling instants, is proposed. It corresponds to the triangular-shaped spectrum developed in Chapter **2**. Potential immunity of the triangular pulse to sampling error relative to that of the raised-cosine pulse is first established. Performance in the presence of jitter of filters designed with the triangular target function is also investigated.

3.1 Introduction

According to the previous chapter, pulse transmission through a band-limited channel without intersymbol interference (ISI) must satisfy the Nyquist condition (2-1). Consequently, the corresponding frequency response satisfies (2-2) and is normally required to be band-limited to frequencies less than some cutoff frequency. These simple time and frequency domain specifications represent the minimum requirements that the filter (primarily a pulse shaping network) must meet [4]. Filter design for data transmission involves the search for functions that satisfy the above time and frequency domain specifications to be used as target functions for filter design such that the resulting filter will be appropriate for a predetermined task, such as reduction of jitter effect.

A widely used class of baseband pulses that satisfy the Nyquist Criterion for eliminating ISI in narrow-band communications are those corresponding to the standard raised-cosine spectrum. An alternative function, one with triangular spectrum, is investigated as a target for filter design. Compared to the raised-cosine function which has zero crossings at the sampling instants, the corresponding time response has zero derivatives at the sampling instants, a desirable property from the point of view of combating the jitter effect.

The objective of this chapter is to use the triangular spectrum developed under the Worst-Case Design Method discussed in Sects. **2.3.1** and **2.3.2**, with roll off factor $\alpha = 1$, as target function for filter design for data transmission through band-limited channels, and compare the jitter performance of the generated pulse to the performance of

the pulse generated with the standard raised-cosine target function.
This treatment has first been presented to the Gradcon'98 [15], and partially in [16].

Examples of the use of the raised-cosine rolloff spectrum as a target function to design filters for data transmission through band-limited channels are designed by the method reported in [6], and a modification is reported in [17]. In the design method, the product of the raised-cosine spectrum and a linear phase polynomial representing the denominator of the transfer function of the filter are used to approximate the corresponding numerator polynomial.

The following section introduces the triangular and the raised-cosine target functions, and their performance in the presence of timing jitter is investigated. The corresponding filter design method is briefly presented in Sect. **3.3**. A filter design example, and actual pulse performance in the presence of timing jitter is presented in Sect. **3.4**. The conclusion is presented in Sect. **3.5**.

3.2 Design Target Functions

The proposed pulse can be expressed as

$$h(t) = \frac{1}{T}\left(\frac{\sin(\pi t/T)}{\pi t/T}\right)^2 = \frac{1}{T}(Sa(\pi t/T))^2 \tag{3-1}$$

where Sa is the sampling function defined as $Sa(x) = \sin x/x$. This is a sinc-squared function or pulse, and will be referred to as the triangular pulse on because it has a triangular-shaped spectrum which is given by

$$H_T(f) = \begin{cases} (1 - T|f|) & |f| \le 1/T \\ 0 & otherwise \end{cases} \tag{3-2}$$

With roll off factor $\alpha = 1$, this is a special case of the spectrum with triangular rolloff function (2-9) derived under the worst-case design criterion of Sect. **2.3.1**. The triangular pulse can be obtained from the expression for generating pulses satisfying the Nyquist criterion given in (2-11) with *roll-off factor* $\alpha = 1$. Compared to the raised-cosine pulse, the proposed pulse has zero derivatives at the sampling instants, and does not cross the time axis, as shown in Fig 3.1.

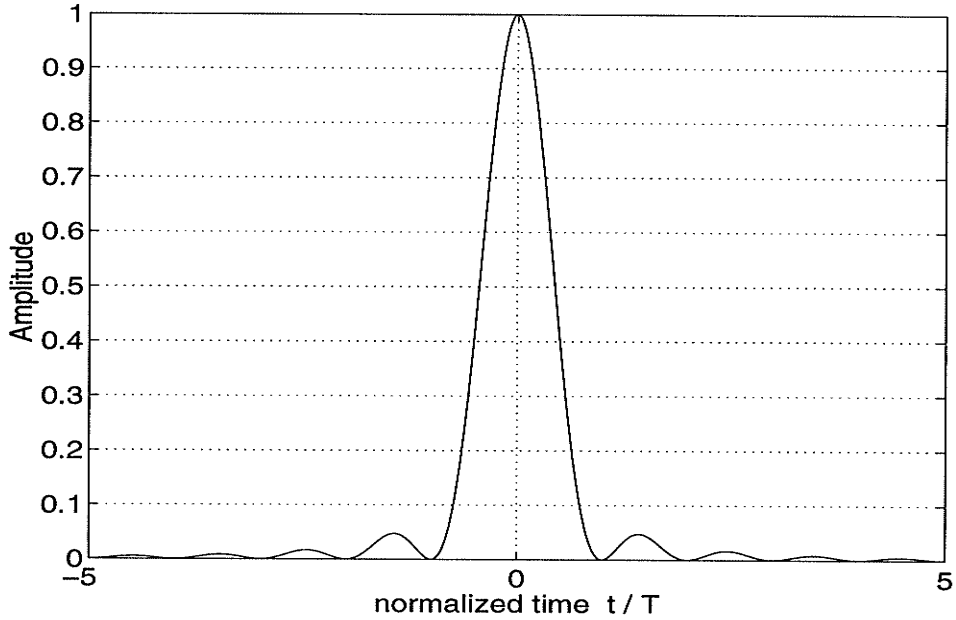

Fig. 3.1 Time response of the triangular rolloff function

As discussed in Sect. **2.4,** this pulse is optimum with respect to timing errors under the LMS design criterion ($\alpha = 1$), and has better performance than the raised-cosine pulse under the LMS design criterion, as well as under the worst-case design criterion.
The second function to be considered for comparison purposes is the standard raised-cosine spectrum (2-4). In contrast to the triangular function (3-1), the pulse corresponding to the raised-cosine spectrum is given by (2-5), it crosses the time axis at the sampling instants, and has sidelobes that decrease with the roll off factor α which assumes values between 0 and 1 (see Fig. 2.1).

The received pulse is to be sampled at integer multiples of the sampling period T. As the sampling instants may not be precisely known at the receiver, the time response of the filter may deviate from zero as the actual sampling instants do not occur at exact multiples of the sampling period, producing a sampling error as jitter effect. Timing jitter is simulated by allowing the sampling instant to vary over part of the sampling period to produce a sampling error, which is evaluated according to the following time-domain formula [6]:

$$Sampling\ \ error = \sum_{\substack{k = -\lfloor k_m \rfloor \\ k \neq 0}}^{\infty} h^2(t_m + kT) \tag{3-3}$$

where h is the normalized impulse response, i. e., $h(t_m) = 1$, t_m is the centre of the main lobe, $k_m = t_m/T$ is the number of zero crossings before the main lobe, and $\lfloor k_m \rfloor$ is the largest integer less than or equal to k_m.

Specifically, to account for the side lobes at the leading and trailing edges, $h(t)$ is evaluated at an array of time instants $(t_m + kT - \tau T \le t \le t_m + kT + \tau T)$, where τ is the timing jitter relative to the sampling period T, or the jitter level.

Using 100% excess bandwidth indicated by $\alpha = 1$ the performance of the raised-cosine pulse, and the triangular pulse (3-1) for jitter levels up to 20% of the sampling period T is shown in Fig. 3.2. Superior performance of the ideal triangular pulse over that of the ideal raised-cosine pulse suggests superiority of the filter designed with the triangular target function over filters designed with the raised-cosine target function. The performance curves shown in Fig. 3.2. are obtained for ideal pulses, so they represent lower bounds on the sampling error that can be achieved by the raised-cosine filter, and the triangular filter, respectively.

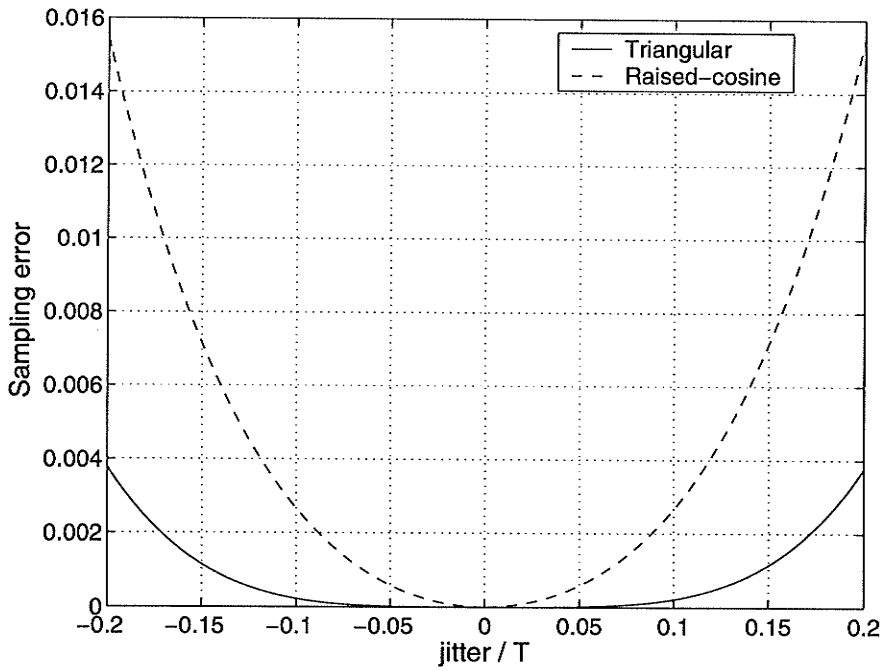

Fig. 3.2 Target performance in the presence of jitter

3.3 The Design Method

The transfer function of the filter can be written as

$$H(j\omega) = \frac{P_m(j\omega)}{Q_n(j\omega)} \cong H_T(j\omega) \tag{3-4}$$

where m is the degree of the numerator polynomial, n is the degree of the denominator polynomial ($m \leq n$), and $H_T(j\omega)$ is a known function with desirable properties whose amplitude is used as a target. The denominator, $Q_n(j\omega)$, of the transfer function is given by a recurrence relation which approximates an equiripple linear phase characteristic of a given order n [18]. Filters of the same degree designed by this method have the same denominator polynomial $Q_n(p)$ regardless of which target function is being used. The deviation from ideal linear phase condition, the phase error, is shown in Fig. 3.3 for an equiripple, linear phase polynomial $Q_8(j\omega)$.

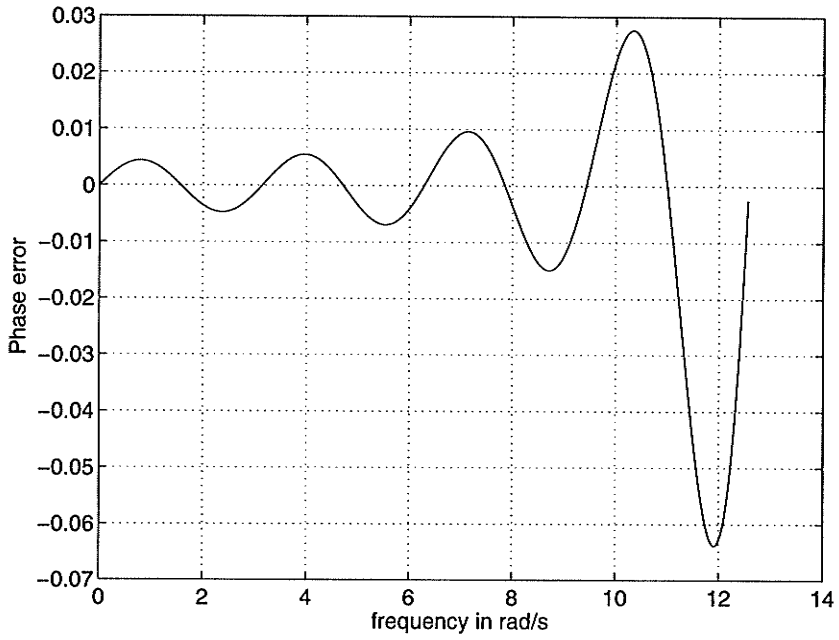

Fig. 3.3 Phase error of the equiripple linear phase polynomial

Rearranging equation (7), the numerator polynomial can be expressed as

$$P_m(j\omega) \cong H_T(j\omega)Q_n(j\omega) \tag{3-5}$$

Briefly described, the design method uses the amplitude of a known function $H_T(j\omega)$ as a target with an imposed linear phase, the design task then is to find the polynomial which fits the product of the target spectrum and the denominator polynomial, which is used to approximate the corresponding numerator polynomial. The coefficients of the numerator polynomial are determined by minimizing the square error signal in the transmission band. A complete account of the design method can be found in [6] and [17].

3.4 Filter Design Example and Performance

The triangular function is used as a design target for an 8th order filter in the modified method [17], with the magnitude-midpoint frequency $\omega_1 = 2\pi$, $T = 1/2$ and the main lobe centre location $\beta = 0.8$. The transfer function of the filter is given in Table 3.1 in zero-pole representation. For 0 dB at $\omega = 0$, the constant factor is $K = 0.015105$. The resulting pulse is contrasted to the ideal triangular pulse in Fig. 3.4. The magnitude and attenuation response of the resulting filter are shown in Fig. 3.5.

Table 3.1: Zeros and poles of transfer function of 8th order filter

Zeros	Poles
424.4781	$-1.5868 \pm j11.4390$
$\pm j12.7572$	$-2.2464 \pm j8.1775$
$4.8791 \pm j5.4909$	$-2.5973 \pm j4.9073$
$-4.8791 \pm j5.4909$	$-2.7564 \pm j1.6359$

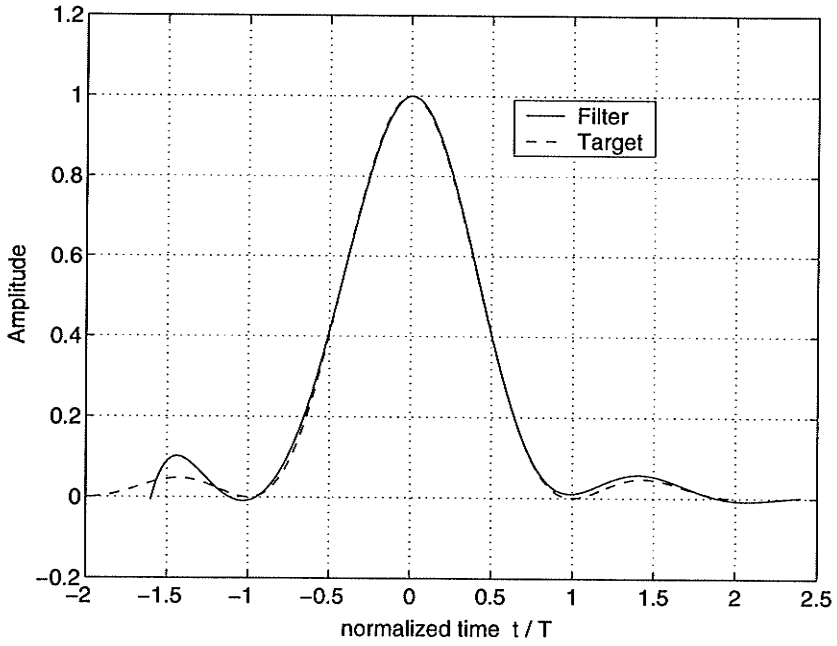

Fig. 3.4 Time response of the triangular filter versus its target function

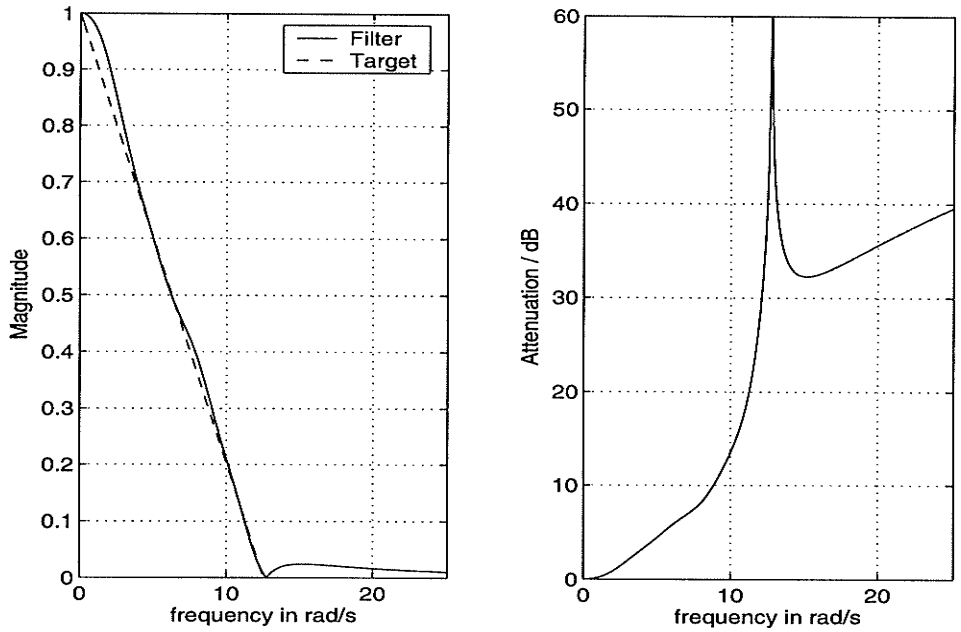

Fig. 3.5 Magnitude and attenuation response of the triangular filter, n=8

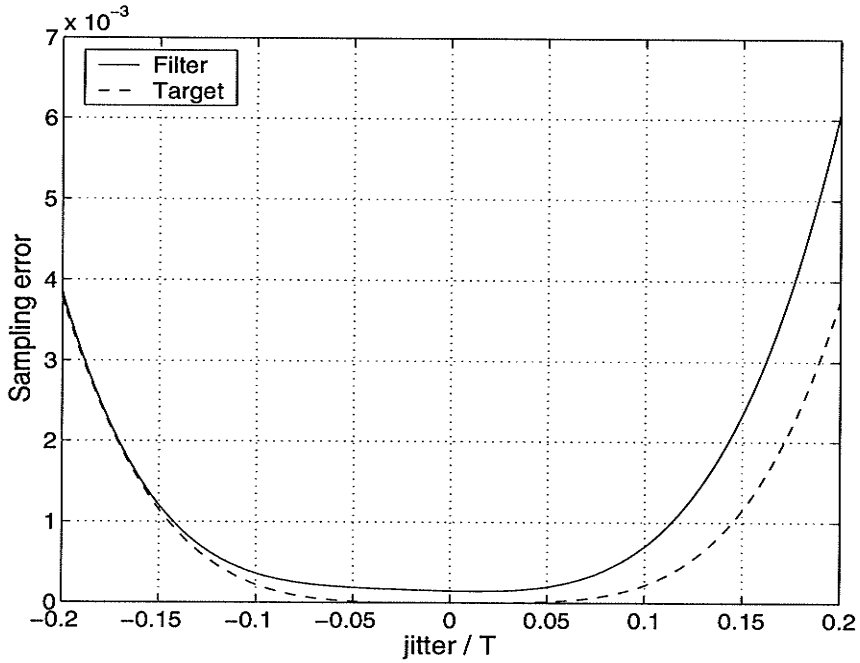

Fig. 3.6 Filter performance in the presence of jitter

The filter performance with respect to jitter compared to that of its target is shown in Fig. 3.6. The performance of the triangular filter is superior to that of the raised-cosine filter since it is superior to the performance of the raised-cosine target itself, which is shown in Fig. 3.2. The sampling error although small is not zero at zero jitter. This is due to the deviation of the leading edge of the filter time response from the ideal case.

To further improve the jitter performance, the sidelobes of the pulse must be attenuated. One way to achieve this is by allowing more bandwidth, another way is to allow more transmission zeros at infinity, i.e., to use a higher degree denominator polynomial which leads to a higher order filter.

3.5 Conclusions

1) Having zero derivatives at the sampling instants, the triangular function has been shown to have better performance in the presence of jitter than the raised-cosine function which has zero crossings at the sampling instants. This result is exploited for designing filters with improved performance in the presence of jitter.

2) An 8th order filter, which is designed using the triangular function as a target, is shown to out perform the raised-cosine target function, and hence out performs the filter designed with the raised-cosine function as a target.

3) The design method does not produce a close fit and the time response of the filter is not close enough to the ideal triangular pulse, consequently, performance of the ideal triangular pulse in the presence of jitter could not be closely achieved by the time response of the designed filter. Better approximation can be achieved with higher order filters. However, this design method suffers from possible computation inaccuracy as the matrix representing the set of linear equations tends to becomes ill conditioned and close to singular.

Chapter 4

Causal Real Symmetric Pulse and Linear Phase Matched Filter Design

Real symmetric pulse transmission under a linear phase condition is presented. The mathematical relationship between the causal real symmetric pulse and the linear phase characteristic is formally proven; it is shown that linear phase is a necessary and sufficient condition for symmetric impulse response. It is also shown that if a causal real symmetric pulse is the input to the channel, it will be matched to a receive filter which is identical to the transmit filter. The delayed raised-cosine pulse is considered for the causal real symmetric Nyquist pulse. A novel design method used to generate a Nyquist pulse with a linear phase polynomial for the denominator of the transfer function and an appropriate placing of the zeros of the numerator is described. The transmission zero pairs are placed on the $j\omega$-axis in accordance with the ideal raised-cosine attenuation response, providing high attenuation in the stopband. The combination of even symmetry of time response, and conjugate transmission zero pairs leads to a linear phase pulse shaping filter which is its own match.

4.1 Introduction

Nyquist pulse shaping can be done completely at the transmitter or the receiver end. This assumes that the other filters in the overall system have only a minor effect on the ISI. Splitting the overall Nyquist filter, primarily a pulse shaping filter, between the transmitter and the receiver is done to compensate for the possible distortion of the channel by matching the receiver to the transmitter. The characterizations of the matched filter were derived by North [19]. Review material on the matched filter and its properties is provided by Turin [20].

To maximize the S/N (signal-to-noise ratio), the transfer function of the Nyquist filter is divided between the transmitter and the receiver, hence giving rise to the transmit and receive filters. Part of the filtering would be carried out at each end of the channel, with each filter contributing half the response, i.e. the division is done symmetrically between the transmitter and the receiver, and the transfer function of each resulting filter is the square root of the transfer function of the overall Nyquist filter, leading to the well known square root filter approach [21].

An alternative approach where the transmit and receive filters have the same magnitude response, while the impulse responses are time-reversed versions of each other is used in this chapter. The receive filter is matched to the transmit filter in this case, and the filtering is optimal for linearly modulated systems when the channel noise is additive white Gaussian noise and there is no ISI in the overall system [22].

The transmitted pulse is contained in the main lobe, and has even symmetry leading to identical transmit and receive filters, which are linear phase. Each of the transmit and receive filters satisfies the Nyquist criterion.

The relationship between the causal real symmetric pulse and the linear phase characteristic is mathematically established in Sect. **4.2**. The continuous time delayed raised-cosine pulse is analyzed as an example of a causal real symmetric pulse in Sect. **4.3,** and an approximation is found using rational functions with linear phase denominator polynomials in Sect. **4.4**. A good approximation to the continuous time delayed raised-cosine pulse is provided in Sect. **4.5** by adding imaginary transmission zero pairs. The matched transmit and receive filter pair is discussed in Sect. **4.5** and design examples in terms of linear phase filters of various orders are given. The conclusions are given in Sect. **4.6**.

4.2 Causal Real Symmetric Impulse Response and Linear Phase

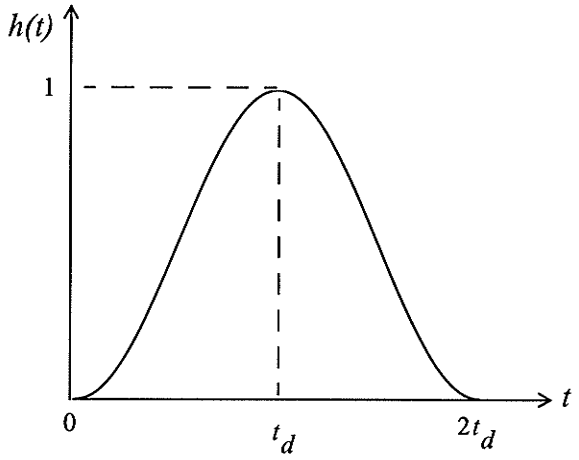

Fig. 4.1 Causal real symmetric pulse

The output of a filter $H(j\omega)$ at the transmitter provides an input signal $h(t)$ to the channel. Assuming a linear channel of sufficient bandwidth so that the input signal $h(t)$ is not changed in shape, this signal –except for additive noise– will also appear at the input of the receive filter. The receive filter is required to be matched to the signal; i.e. its impulse response has the same shape as $h(t)$ but is reversed in time and shifted by $2t_d$, where t_d is the time delay between the pulse arrival and the output peak, that is the time to peak. Thus the impulse response of the receive filter is $h(-t+2t_d)$.

Furthermore, the causal real symmetric pulse shown in Fig. 4.1 satisfies the equality

$$h(t) = h(-t+2t_d)$$

It follows that

$$\mathcal{F}\{h(t)\} = H(j\omega) = \mathcal{F}\{h(-t+2t_d)\}$$

$$H(j\omega) = \int_{-\infty}^{\infty} h(-t+2t_d)\ e^{-j\omega t}\ dt$$

$$H(j\omega) = \int_{-\infty}^{\infty} h(\tau)\ e^{-j\omega(2t_d-\tau)}\ d\tau = e^{-j\omega 2t_d}\int_{-\infty}^{\infty} h(\tau)\ e^{j\omega\tau}\ d\tau$$

where the last equality is obtained by substituting $\tau = 2t_d - t$.

Therefore

$$H(j\omega) = e^{-j\omega 2t_d}H(-j\omega) = e^{-j\omega 2t_d}H^*(j\omega) \qquad (4\text{-}1)$$

where the fact that $H^*(j\omega) = H(-j\omega)$ for a real impulse response $h(t)$ has been used in (4-1). The frequency response of the matched filter is the complex conjugate of the transmitted spectrum multiplied by a phase factor representing the sampling delay of $2t_d$.

Equation (4-1) can be written as

$$H(j\omega)e^{j\omega t_d} = H^*(j\omega)e^{-j\omega t_d} = (H(j\omega)e^{j\omega t_d})^*$$

Thus, the quantity $H(j\omega)e^{j\omega t_d}$ is real, and $H(j\omega) = |H(j\omega)|e^{-j\omega t_d}$.

The transfer function $H(j\omega)$ with real impulse response $h(t)$, which is symmetric about t_d can be expressed as $H(j\omega) = |H(j\omega)| \cdot \exp(j\phi(j\omega))$, where $|H(j\omega)|$ is real-valued with even symmetry, and $\phi(j\omega)$ is real-valued with odd symmetry. Specifically, $\phi(j\omega) = -\omega t_d$. Assume that $h(t)$ is symmetric about t_d and causal, then $h(t) = 0$ for $t < 0$ and $t \geq 2t_d$. It follows that $h(t) = h(-t + 2t_d)$, which is the condition for a matched filter in this case. Thus $H(j\omega)$ is its own match, and using a pulse shaping filter $H_{Tx}(j\omega) = H(j\omega)$ at the transmitter, the receive filter is given by $H_{Rx}(j\omega) = H(j\omega)$. Note that $h(t)$ is the input pulse of the receive filter, which is identical to the transmit filter, the total delay of the transmit and receive filter combination is $2t_d$

Real causal symmetric impulse response (such as the one shown in Fig. 4.2b) leads to a novel design of the matched filter, and is equivalent to a linear phase response as proved by the following theorem.

THEOREM 4.1:

The real impulse response $h(t)$ is symmetric if and only if the phase $\angle H(j\omega)$ is linear.

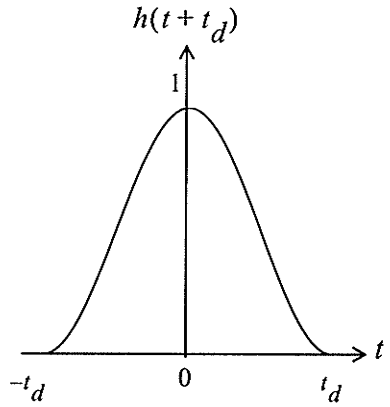

Fig. 4.2a Real symmetric pulse

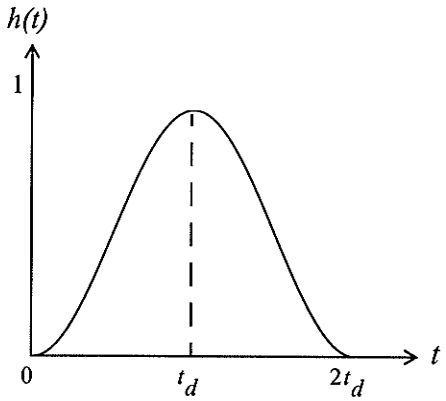

Fig. 4.2b Real delayed symmetric pulse

Proof:

Assuming even symmetry of $h(t)$ about t_d, implies $h(t+t_d) = h(-t+t_d)$.

$$H(j\omega) = \int_{-\infty}^{\infty} h(t)\ e^{-j\omega t}\ dt$$

Replacing t by $t+t_d$

$$H(j\omega) = \int_{-\infty}^{\infty} h(t+t_d)\ e^{-j\omega(t+t_d)}\ dt$$

It follows that

$$H(j\omega) = e^{-j\omega t_d} \int_{-\infty}^{\infty} h(-t+t_d)\ e^{-j\omega t}\ dt$$

Let $\tau = -t + t_d$, then

$$H(j\omega) = e^{-j\omega t_d} \int_{-\infty}^{\infty} h(\tau)\ e^{-j\omega(t_d-\tau)}\ d\tau$$

$$= e^{-j\omega 2t_d} \int_{-\infty}^{\infty} h(\tau)\ e^{j\omega\tau}\ d\tau = e^{-j2t_d\omega}\ H(-j\omega)$$

and

$$\angle H(j\omega) = -2t_d\omega + \angle H(-j\omega)$$

Since the phase $\angle H(j\omega)$ is odd for real $h(t)$, $\angle H(j\omega) = -\angle H(-j\omega)$, we then have

$$\angle H(j\omega) = -t_d\omega \tag{4-2}$$

and the phase $\angle H(j\omega)$ is linear.

Therefore, linear phase is necessary for an even symmetric impulse response $h(t)$.

To prove the sufficiency condition, assume a linear phase

$$\angle H(j\omega) = -t_d\omega,\ t_d > 0$$

then

$$H(j\omega) = |H(j\omega)|\angle H(j\omega) = |H(j\omega)|e^{-j\omega t_d}$$

It is required to show that the real impulse response $h(t)$ is symmetric, that is

$$h(t + t_d) = h(-t + t_d).$$

The impulse response can be expressed in terms of the inverse Fourier transform relation:

$$h(t) = \frac{1}{2\pi}\int_{-\infty}^{\infty} H(j\omega)\ e^{j\omega t}\ d\omega$$

Then with t replaced by $t + t_d$

$$h(t+t_d) = \frac{1}{2\pi}\int_{-\infty}^{\infty} H(j\omega)\ e^{j\omega(t+t_d)}\ d\omega$$

$$= \frac{1}{2\pi}\int_{-\infty}^{\infty} |H(j\omega)|e^{-j\omega t_d}\ e^{j\omega(t+t_d)}\ d\omega$$

$$= \frac{1}{2\pi}\int_{-\infty}^{\infty} |H(j\omega)|\ e^{j\omega t}\ d\omega$$

The magnitude function is even, $|H(j\omega)| = |H(-j\omega)|$ for a real pulse, therefore

$$h(t+t_d) = \frac{1}{2\pi}\int_{-\infty}^{\infty} |H(-j\omega)|\ e^{j\omega t}\ d\omega$$

$$= \frac{1}{2\pi}\int_{-\infty}^{\infty} |H(-j\omega)|e^{j\omega t_d}\ e^{j\omega(t-t_d)}\ d\omega$$

$$= \frac{1}{2\pi}\int_{-\infty}^{\infty} H(-j\omega)\ e^{j\omega(t-t_d)}\ d\omega$$

Replacing ω by $-\omega$

$$h(t+t_d) = \frac{1}{2\pi}\int_{-\infty}^{\infty} H(j\omega)\ e^{j\omega(-t+t_d)}\ d\omega$$
$$= h(-t+t_d)$$

implying that $h(t)$ is symmetric about t_d, and thus a linear phase is necessary and sufficient for the impulse response $h(t)$ to be symmetric.□

A causal symmetric pulse is necessarily of finite duration as can be seen from Fig. 4.2b, where the pulse is contained within the interval $[0,\ 2t_d]$.

The Fourier transform relation in this case reduces to

$$H(j\omega) = \int_0^{2t_d} h(t)\ e^{-j\omega t}\ dt$$

Replacing t by $\tau + t_d$ advances the pulse as shown in Fig. 4.2a

$$H(j\omega) = \int_{-t_d}^{t_d} h(\tau + t_d)\ e^{-j\omega(\tau + t_d)}\ d\tau$$

It follows that

$$H(j\omega) = e^{-j\omega t_d} \int_{-t_d}^{t_d} h(\tau + t_d)\ e^{-j\omega\tau}\ d\tau$$

The magnitude is obtained by taking the absolute value on both sides

$$|H(j\omega)| = \left| \int_{-t_d}^{t_d} h(\tau + t_d)\ e^{-j\omega\tau}\ d\tau \right|$$

$$|H(j\omega)| = 2\left| \int_{0}^{t_d} h(\tau + t_d)\cos(\omega\tau) d\tau \right| \qquad (4\text{-}3)$$

Given a desired pulse shape $h(t)$, the target function for filter design $|H(j\omega)|$ can be generated using a simple integral relation (4-3).

The scaling factor is given by $H(0) = 2\int_0^{t_d} h(\tau + t_d)\ d\tau$.

4.3 The Time-Domain Raised-Cosine Pulse

A real pulse which if delayed by t_d has even symmetry about the point t_d is the time-domain raised-cosine pulse, given by

$$p_{rc}(t) = \begin{cases} \frac{1}{2}(1 + \cos(\pi t / t_d)) & |t| \le t_d \\ 0 & otherwise \end{cases} \tag{4-4}$$

Note that this name 'raised-cosine' is often used to refer to the pulse with a raised-cosine rolloff spectrum, that is a raised-cosine in the frequency domain, which is also referred to as the standard raised-cosine pulse or the raised-cosine spectrum pulse. The time-domain raised-cosine pulse of (4-4) shown in Fig. 4.3 will be referred to simply as the raised-cosine pulse. Also, the word pulse will be used in the foregoing discussion to mean the time response, and whether it is the impulse response or the response to a pulse input should be clear from the context. However, in most cases it is the impulse response.

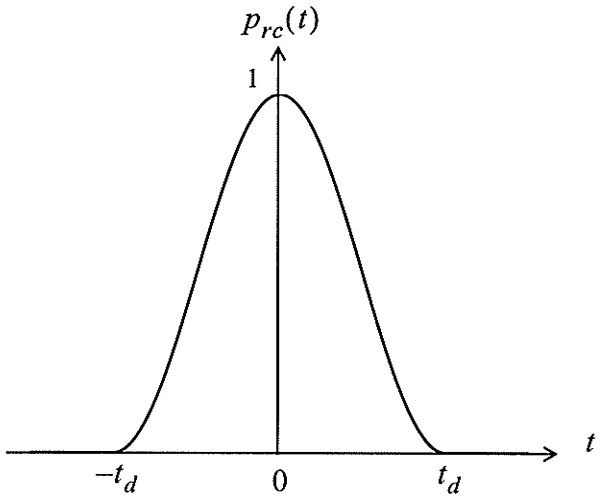

Fig. 4.3 The time-domain raised-cosine pulse

If delayed by t_d, the raised-cosine pulse becomes causal, it has even symmetry about t_d and is contained within the main lobe $[0,\ 2t_d]$, as shown in Fig. 4.1. Thus by *Theorem 4.1*, this delayed version has a linear phase or equivalently a constant delay t_d. The raised-cosine pulse is discussed in [23] in relation to the Squaring Synchronizer for PAM signals which is used to generate a spectral line clock synchronizer. However, the motivation for considering the raised-cosine pulse in the context of matched filter design is based on the discussion of Sect. **4.2** that if this symmetric pulse is used as the input to the channel, i.e. is the output of the shaping filter at the transmitter, the causal raised-cosine pulse will be matched to a receive filter which is identical to the transmit filter.

The spectrum corresponding to the raised-cosine pulse with unity maximum amplitude can be expressed as

$$P_{rc}(f) = t_d S_a(2\pi f t_d) + \frac{t_d}{2} S_a(2\pi f t_d + \pi) + \frac{t_d}{2} S_a(2\pi f t_d - \pi) \qquad (4\text{-}5)$$

where $S_a(x) = \sin(x)/x$. This spectrum is real and the phase is zero.

The frequency domain representation of the raised-cosine pulse given by (4-5) with $t_d = 1$ indicates that there are transmission zero pairs at integer multiples of π starting at 2π. This is clearly indicated by Fig. 4.4 which shows the ideal attenuation response of the raised-cosine pulse versus frequency f for the case $t_d = 1$, or in general versus ft_d.

The raised-cosine pulse has transmission zero pairs at

$$s = j\omega = \pm jk\pi t_d, \quad k = 2,3,4,\ldots \qquad (4\text{-}6)$$

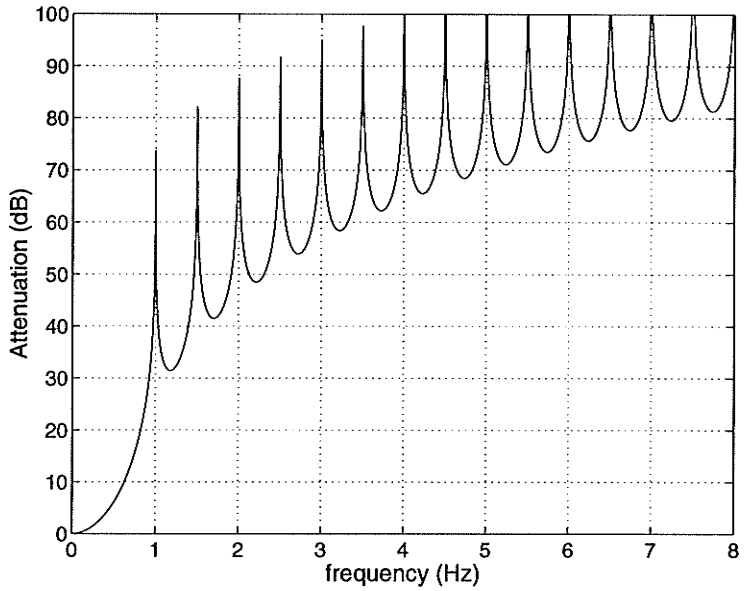

Fig. 4.4 Ideal raised-cosine attenuation response

4.4 Rational Function Approximation of the Causal Raised-Cosine Pulse without Transmission Zeros

According to *Theorem 4.1*, of Sect. **4.2**, the causal raised-cosine pulse, due to its even symmetry, can be approximated by the impulse response of an approximately linear phase filter. The transfer function of a filter of order n can be written as

$$H(s) = \frac{P_m(s)}{Q_n(s)} \tag{4-7}$$

where m is the degree of the numerator polynomial, n is the degree of the denominator polynomial ($m \leq n$), and s is the complex frequency variable.

The denominator $Q_n(s)$ of the transfer function of the filter is a linear phase polynomial of degree n, which is generated by the following recurrence relation [24]:

$$Q_1(s) = s + 1$$

$$Q_2(s) = s^2 + 3s + 3$$

$$Q_{n+1}(s) = (2n+1)Q_n(s) + s^2 Q_{n-1}(s), \quad n = 2, 3, \ldots \tag{4-8}$$

Equivalently, the coefficients of the polynomial $Q_n(s) = \sum_{k=0}^{n} b_k s^{n-k}$ are given in closed form by

$$b_k = \frac{\binom{n}{k}}{\binom{2n}{k}} \frac{2^k}{k!} \tag{4-9}$$

Derivation of the above relations is based directly on phase linearity, more details can be found in Appendix **A4**.

A polynomial which is derived for maximally flat delay, is expressed as [25]:

$$Q_n(s) = \sum_{k=0}^{n} \frac{(n+k)!\, s^{n-k}}{k!(n-k)!\, 2^k} \tag{4-10}$$

Any one of (4-8), (4-9), and (4-10) can be used for a linear phase, constant delay polynomial, and each polynomial produces a unity nominal delay which can be changed through frequency scaling.

To approximate the causal raised-cosine pulse shown in Fig. 4.1 and produce a pulse with even symmetry, a linear phase polynomial $Q_n(s)$, as given by (4-8) is used in the denominator of a transfer function with a unity numerator polynomial ($P_m(s) = 1$). The time response of such a transfer function is shown in Fig. 4.5 for $n = 7$, 8, and 9, where n is the degree of the denominator polynomial.

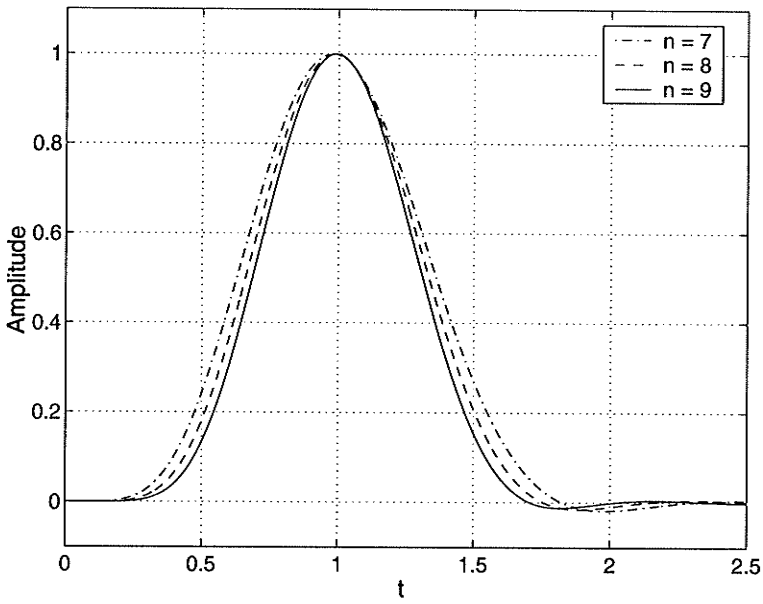

Fig. 4.5 Linear phase time response

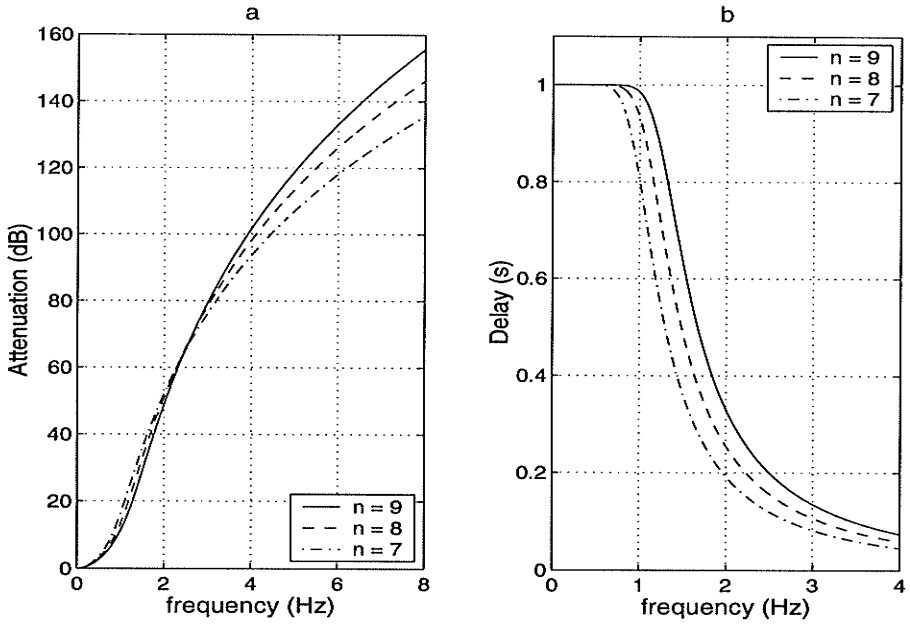

Fig. 4.6 Attenuation and delay frequency response

The pulse represented by this time response is essentially contained within the main lobe ($t \in [0, 2]$), and will be referred to as the causal real symmetric (CRS) pulse. This pulse becomes narrower with increased order n.

The attenuation and delay response are shown in Fig. 4.6a and Fig. 4.6b, respectively. The delay response is solely determined by the denominator polynomial, the flat part of the delay response is unity and extends over a wider frequency range for increased order n. In fact, all responses are determined by the denominator polynomial in case of a unity numerator polynomial.

The attenuation response of Fig. 4.6a has no pronounced stopband edge, it can be made to approximate the causal raised-cosine attenuation response by equivalently approximating the ideal attenuation response of the raised-cosine pulse by using a numerator polynomial which has finite transmission zero pairs at $\pm jk\pi$, $k = 2,3,4,\ldots,m$, as indicated by Fig. 4.4. Note that $t_d = 1$ in this case and for a rational transfer function H, the integer m satisfies $m \leq n$.

4.5 Rational Function Approximation of The Causal Raised-Cosine Pulse with Transmission Zeros

The next step is to include transmission zeros in the numerator of the transfer function, and the filter transfer function (4-7) becomes

$$H(s) = \frac{P_m(s)}{Q_n(s)} = K\prod_{k=1}^{m/2}(s^2+\omega_k^{\,2})/\prod_{k=1}^{n}(s-p_k) \qquad (4\text{-}11)$$

where m is the degree of the numerator polynomial, necessarily even, n is the degree of the denominator polynomial ($m \le n$), K is a real constant, $j\omega_k$ are imaginary zeros and p_k are the poles in the left-half s-plane, and s is the complex frequency variable.

The transfer function of the filter is developed with imaginary zeros, enabling filter implementation in terms of ladder LC networks, with high stopband attenuation and low component sensitivity. Moreover, LC ladder network models translate to active models, so are useful prototypes for active filters as well as for Wave Digital filters.

To approximate the ideal raised-cosine attenuation response shown in Fig. 4.4 one transmission zero pair at $\pm j2\pi$ is added to the numerator of the transfer function of the previous section, but this does not produce an impulse response with good symmetry, so a second pair is added at $\pm j3\pi$. The resulting attenuation and time response are shown in Fig. 4.7, and Fig. 4.8, respectively. Observe the symmetry of the resulting response, an essential feature if this response is to be considered as the output of the transmit filter and the input pulse for the receive filter. Adding a third pair at $\pm j4\pi$ produces a less symmetric impulse response, with unacceptable behaviour at $t = 0$ for $n = 7$.

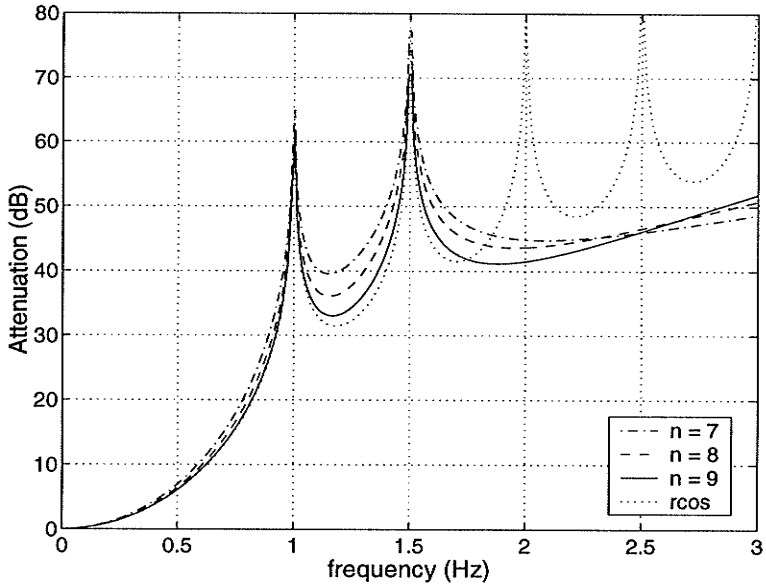

Fig. 4.7 Linear phase approximation to the raised-cosine: attenuation response

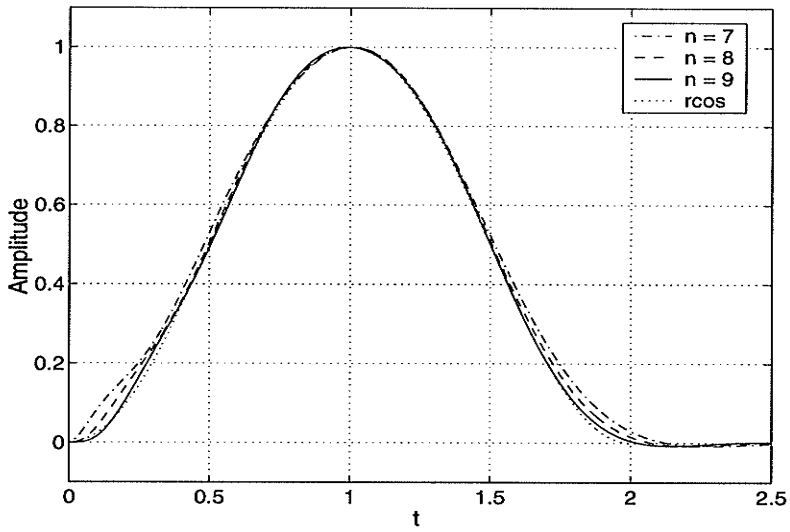

Fig. 4.8 Linear phase approximation to the raised-cosine: impulse response

The zeros and poles of the resulting transfer function are given in Table 4.1 for n=7, 8 and 9. For 0 dB at $f = 0$, the constant factor is K= 38.5359 for n=7, K= 578.0390 for n=8, and K= 9826.6624 for n=9.

Table 4.1: Zeros and poles of filter transfer function

Zeros	Poles, n=7	Poles, n=8	Poles, n=9
$\pm j2\pi$	-2.6857 $\pm j$ 5.4207	-2.8390 $\pm j$ 6.3539	-2.9793 $\pm j$ 7.2915
$\pm j3\pi$	-4.0701 $\pm j$ 3.5172	-4.3683 $\pm j$ 4.4144	-4.6384 $\pm j$ 5.3173
	-4.7583 $\pm j$ 1.7393	-5.2048 $\pm j$ 2.6162	-5.6044 $\pm j$ 3.4982
	-4.9718	-5.5879 $\pm j$ 8676	-6.1294 $\pm j$ 1.7378
			-6.2970

The output pulse of the transmit filter is the pulse going into the channel or the transmitted pulse and it could be any of the pulses shown in Fig. 4.8. However, the pulse with $n = 9$ is used in the following discussion of the transmit and receive matched filter pair. The output of the receive filter is the pulse response of the receive filter to the transmitted pulse. Equivalently, the output of the receive filter can be obtained as the impulse response of the cascade of two identical filters, the transmit filter and the receive filter. The overall transfer function has double the transmission zero pairs, as well as double the poles of the transmit filter. The resulting attenuation response is shown in Fig. 4.9 which indicates that the cascade of the transmit filter and the receive filter achieve a minimum stopband attenuation of 66 dB.

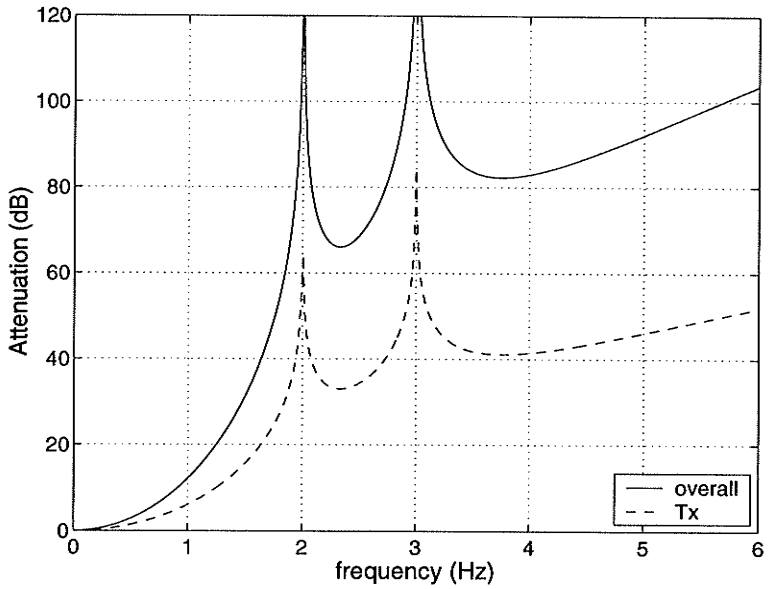

Fig. 4.9 Attenuation response corresponding to n= 9

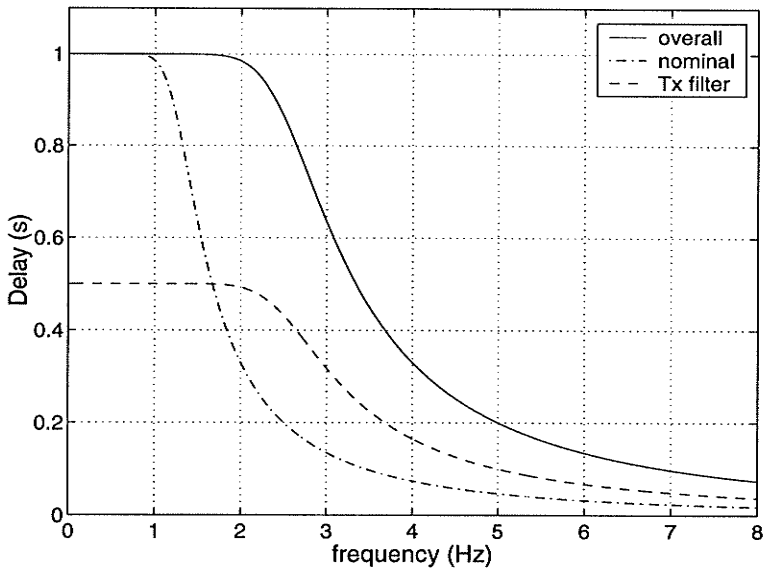

Fig. 4.10 Delay response corresponding to n= 9

The resulting delay response is shown in Fig. 4.10; the nominal unity delay curve is for the transfer function before scaling. To sample the output pulse of the receive filter every $T = 1$, the transfer function is scaled by a factor of 2 generating a narrower transmitted pulse which corresponds to the lower delay curve with a flat part of 0.5 (dashed line). The solid curve represents the total delay of the system, which is flat for twice the range of the nominal curve. The output pulse of the receive filter is shown in Fig. 4.11; it is the impulse response of the cascade of the transmit and receive filters.

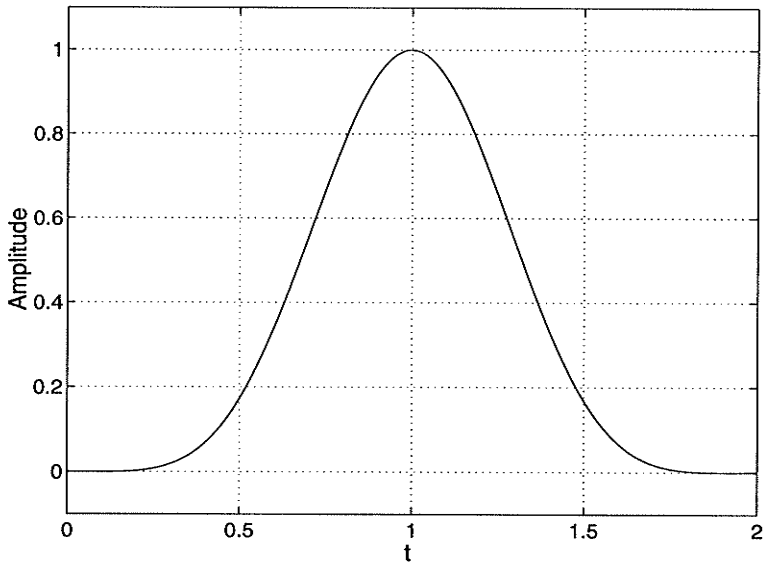

Fig. 4.11 Receive filter output pulse, n= 9

Symmetry of the transmitted pulse is important for the validity of the foregoing design, and as Fig. 4.8 indicates, the linear phase design generates a pulse with good symmetry. However, immunity of the receive filter output pulse to timing jitter is ultimately important. Since the transmit and receive filters are identical, the receive filter output pulse is the convolution of the transmitted pulse with itself. The received pulse is flatter than the transmitted pulse with negligibly small amplitude at and near the end points, $t = 0$ and

$t = 2T$. This improves jitter performance. The sampling error is less than $6x10^{-6}$ for jitter levels up to 20% of the sampling period T. Note that the sampling error for the raised-cosine spectrum pulse reaches 0.01548 for the same jitter levels. Frequency scaling has no effect on pulse symmetry or jitter performance.

4.6 Conclusions

1) Real symmetric pulse transmission under a linear phase condition is presented; it is shown that if a causal real symmetric pulse (such as the time-domain raised-cosine pulse) is the input to the channel, it will be matched to a receive filter which is identical to the transmit filter.

2) Linear phase is necessary and sufficient for the impulse response $h(t)$ to be symmetric. A transfer function with a linear phase denominator polynomial, and $j\omega$-axis transmission zeros is used to approximate the time-domain raised-cosine pulse.

3) The linear phase denominator polynomial generates a pulse with good symmetry which is essentially contained within the main lobe ($t \in [0, 2]$).

4) Even pulse symmetry, and conjugate transmission zero pairs lead to a linear phase pulse shaping filter which is its own match. It can perform both tasks of transmit and receive filter, which can be advantageous in situations where the transmitter and receiver are at the same physical location.

5) A 9th order transmit and the receive matched filter combination achieve a minimum stopband attenuation of 66 dB. Performance of the received pulse in the presence of jitter is quite satisfactory, and the sampling error is virtually zero.

Chapter 5

Causal Real Symmetric Nyquist Pulse Design

The linear phase design method used to generate the causal real symmetric Nyquist pulse of Chapter **4** is discussed further. The maximum number of transmission zero pairs which guarantees zero pulse amplitude at $t = 0$ is derived in terms of the filter order n. Various design aspects are thoroughly investigated, using the least-mean-square (LMS) timing error and the jitter performance of the pulse as figures of merit. A pulse symmetry factor is also defined and used. Practical design examples show that the generated pulse has negligible energy outside the mainlobe and better jitter performance than the LMS pulse as well as the raised-cosine spectrum pulse. A transfer function realization as a ladder LC network is given. An algorithm for placing the zeros of the numerator to produce an attenuation response of arbitrary shape is described and an example is given. The design method is flexible, robust, and produces practical filters.

5.1 Introduction

The triangular rolloff spectrum (Sect. **3.2**) and the spectrum corresponding to the optimum pulse (Sect. **2.4**) are theoretical results that cannot be produced exactly in practice as practical filters do not have infinite attenuation over the entire stopband, and the filter necessarily cannot be strictly bandlimited. A practical pulse design has been discussed in Chapter **3** for the triangular pulse using a design method from the literature. It was then noted that the design method does not produce close approximation to the ideal triangular pulse, and that the side lobes of the resulting pulse must be further attenuated to improve jitter performance.

An alternative approach uses a linear phase design to generate a Nyquist pulse with extremely reduced sidelobes, which improves the jitter performance [26]. The resulting pulse is of finite duration and its energy is essentially contained within the main lobe. A design method based on linear phase has been introduced in Chapter **4** where it was used to approximate the time-domain raised-cosine pulse. The linear phase design is investigated further in this chapter, and some special cases are discussed. The transmission zero pairs used in the linear phase designs presented in Chapter **4** were integer multiples of π. These will be adjusted for higher attenuation and better pulse symmetry. The parameters affecting the design are discussed in detail in Sect. **5.2** where a symmetry factor is introduced to quantify pulse symmetry. Pulse design examples are presented in Sect. **5.3**, where the LMS timing error expression of Chapter **2** is used to evaluate the performance of the resulting pulse. The performance of the resulting pulse in the presence of

timing jitter is compared to that of the raised-cosine spectrum pulse, the triangular pulse and the LMS optimum pulse. Unlike the transmit filter design discussed in Sect **4.5**, the linear phase denominator polynomial is not scaled. The delay is $T = 1$ in this case, and the pulse duration is $2T$. An LC pulse shaping ladder network realization is given in Sect. **5.4**. In Sect. **5.5**, an algorithm for placing the zeros of the numerator is described, and used to produce an attenuation response example of arbitrary shape.

The conclusions are presented in Sect. **5.6**.

5.2 Linear Phase Design of the Nyquist Pulse

The transfer function of the filter is given by (4-11), and is repeated here for convenience:

$$H(s) = \frac{P_m(s)}{Q_n(s)} = K \prod_{k=1}^{m/2} (s^2 + \omega_k{}^2) / \prod_{k=1}^{n} (s - p_k) \qquad (5\text{-}1)$$

where m is the degree of the numerator polynomial, n is the degree of the denominator polynomial ($m \le n$), K is a real constant, the transmission zero pairs are $\pm j\omega_k$ and the degree of the numerator polynomial m is an even integer in this case. The p_k are the poles in the left-half s-plane, and s is the complex frequency variable.

The denominator of the transfer function (5-1) is a linear phase polynomial given by (4-8) or (4-9), or equivalently a maximally flat delay polynomial given by (4-10).

The filter has linear phase and maximally flat delay, and its time response is causal, real and symmetric and will be referred to as the causal real symmetric (CRS) pulse.

We are interested in filter design with a low order which can be implemented with few elements leading to a compact design. Ideally, the desired pulse shape is contained within the main lobe and has zero value at the end points $t = 0$ and $t = T$.

The objective is two fold:

1) To generate a practical pulse which is essentially contained within the main lobe and with negligibly small amplitude at and near the end points.

2) To achieve maximum attenuation in the stopband using the least filter order n.

The time domain part of the above objective is motivated by the desire to have a pulse with better performance in the presence of jitter than the raised-cosine spectrum pulse (the standard raised-cosine pulse).

The design figures of merit are the LMS timing error and the jitter performance of the pulse, relative to that of the raised-cosine spectrum pulse with a rolloff factor $\alpha = 1$. The LMS timing error for the raised-cosine spectrum pulse is expressed in terms of the rolloff factor α in (2-25), and jitter was discussed in Sect. **3.2**. As the linear phase filter is expressed in terms of the poles and zeros of its transfer function, we do not have an analytical expression for the LMS rolloff function $Q(f)$ that can be used to derive the expressions of the LMS errors corresponding to the CRS pulse. However, an array of values for the rolloff function can be defined for any value of the rolloff factor α by the relation

$$Q(f) = |H(j2\pi f)|, \quad 1/2T \le f < (1+\alpha)/2T. \tag{5-2}$$

where $|H(j2\pi f)|$ is the magnitude function of the linear phase filter. The LMS timing error can then be calculated for the CRS pulse using the integral relation (2-20).
For the second figure of merit, timing jitter is simulated as a small timing offset and the extreme value that the residual ISI can assume is calculated for the CRS pulse and the raised-cosine spectrum pulse with $\alpha = 1$ using (3-3).

The importance of symmetry of the transmitted pulse for the validity of the foregoing design was stated in Sect. **4.5**, but was not quantitatively developed. To quantify symmetry of the impulse response for various filter orders, a symmetry factor is calculated according to the formula:

$$Symmetry\ \ Factor = \sum_{k=1}^{\lceil N/2 \rceil} |h(k) - h(N-k+1)| / |h(k) + h(N-k+1)| \tag{5-3}$$

where N is the number of impulse response samples. The symmetry factor is ideally zero, but is a positive number for a practical pulse.

As an initial investigation, linear phase filters of various orders (3 to 12) are designed according to (5-1), using a linear phase polynomial (4-8), or (4-9) for the denominator of the transfer function, and a pair of transmission zeros at $f = 1$ for the numerator (one transmission zero pair at $\pm j2\pi$ corresponding to a rolloff factor $\alpha = 1$). It is found that an order 7 filter is the least order filter which generates an acceptable pulse that outperforms the raised-cosine spectrum pulse in terms of jitter and the LMS errors.

Lower order filters allow for transmission zeros at infinity (1 to 4 for filter orders 3 to 6, respectively) but do not generate an acceptable pulse or jitter performance. The simulation result for filters of order 7, 8, 9, and 10 is summarized in Table 5.1, where the last two rows show the LMS timing error and the jitter performance for $\alpha = 1$ and jitter $=0.2T$. Besides the filter order n and minimum stopband attenuation A_s, other quantities of interest for the CRS pulse design are delay droop (decline from unity) at $f = 1$ and bandwidth with flat delay response. Both are determined by the linear phase denominator polynomial and its order n. Simulations are carried out with an actual accuracy of only 4 digits beyond the decimal point. From Table 5.1 the following can be observed:

1) The delay response which depends only on the denominator polynomial improves with higher order n and the flat part extends over a wider frequency range (first two rows of Table 5.1).

2) The LMS timing error generally improves with higher order n, however the minimum attenuation A_s does not.

3) The pulse shape improves with increased number of transmission zeros at infinity which occurs with increased order n; but this situation is no longer true for $n > 9$ indi-

cating that there is a relation between the number of finite transmission zeros and the number of transmission zeros at infinity, in the sense that the latter cannot be increased while keeping the former constant without adverse effect on the pulse shape.

Higher order filters (with one pair of transmission zeros) allow more transmission zeros at infinity but generate an unacceptable pulse shape and low values for A_s.

Higher order filters, n=9 to 15, were investigated using an additional pair of transmission zeros at $\pm j4\pi$, and it was concluded that the jitter performance is best at n=9.

Filter design for higher order would produce a flat delay over a wider frequency range due to a higher degree linear phase denominator polynomial, and higher stopband attenuation as there would be more transmission zeros, however, we are interested in filter design with a low order n.

Table 5.1: Linear phase design quantities

Order n	7	8	9	10
Delay droop at $f = 1$	0.1930	0.06486	0.01413	0.00219
BW at 1% delay droop (Hz)	0.7010	0.8364	0.9718	1.115
Attenuation at 1% delay droop (dB)	12.96	19.22	35.59	24.68
Minimum attenuation A_s (dB)	31.06	27.46	24.01	21.05
Frequency at A_s (Hz)	1.243	1.243	1.259	1.298
Symmetry factor	1.555	1.803	1.827	1.737
Relative LMS timing error	0.5695	0.2329	0.1278	0.1466
Relative jitter performance	0.3284	0.09266	0.02519	0.02690

The CRS pulse design is based on the following observations:

1) The denominator of the transfer function of the filter which is a linear phase polynomial solely determines the pulse shape if the numerator is 1, i. e., there are no finite transmission zeros.

2) Finite transmission zeros –in conjugate imaginary pairs– are required to boost the attenuation at the beginning of the stopband, but once added to the numerator polynomial they can have an adverse effect on the pulse shape.

3) Transmission zeros are needed at infinity to improve the pulse shape.

This means that there is a minimum order n below which the pulse shape is not acceptable. This is best approached through establishing a relation between the filter order n and the number of finite transmission zero pairs $m/2$, which guarantees a zero value for the pulse at $t = 0$.

The condition that $m < n$, although necessary, is not sufficient to guarantee an impulse response with good symmetry.

The number of finite transmission zero pairs $m/2$ allowed for a given filter order n can be derived from the requirement that the pulse amplitude is zero at $t = 0$.

This is done by use of the initial value theorem:

$$h(0^+) = \lim_{s \to \infty} sH(s)$$

Therefore, $h(0^+) = 0$ if and only if $\lim_{s \to \infty} sH(s) = 0$, i.e. a rational function

$H(s) = \dfrac{P_m(s)}{Q_n(s)}$ must have degree of $P_m \leq$ degree of $Q_n - 2$.

If the degree of $Q_n = n$, and the degree of $P_m = 2\nu$ (ν transmission zero pairs on the $j\omega$-axis), then

$$\nu \le \begin{cases} \dfrac{n-3}{2}, & n-odd \\ \dfrac{n-2}{2}, & n-even \end{cases} \tag{5-4}$$

For example, the number of transmission zero pairs, given $n = 7$, cannot exceed 2.

In terms of the figures of merit listed in the last 3 rows of Table 5.1, best pulse symmetry is attained when $n = 7$, however, when $n = 9$ the pulse is narrower and has the best jitter performance. It also has the lowest LMS errors as a received pulse.

5.3 Linear Phase Design Examples

A transfer function is constructed using a 7th degree linear phase polynomial for the denominator and two pairs of finite transmission zeros which, according to (5-4), is the maximum number of finite transmission zero-pairs for $n = 7$. Starting with a set of transmission zero pairs at $\pm j2\pi$ and $\pm j4\pi$, the transmission zeros are adjusted such that the pulse amplitude at $t = 2T$ is reduced. The zeros and poles of the resulting transfer function are given in Table 5.2, and for 0 dB at $f = 0$, the constant factor is K= 15.8171. The resulting attenuation response is shown in Fig. 5.1; the corresponding pulse and the LMS timing optimum pulse are shown in Fig. 5.2. This set achieves a minimum stopband attenuation of 37.6 dB (column 2, Table 5.4).

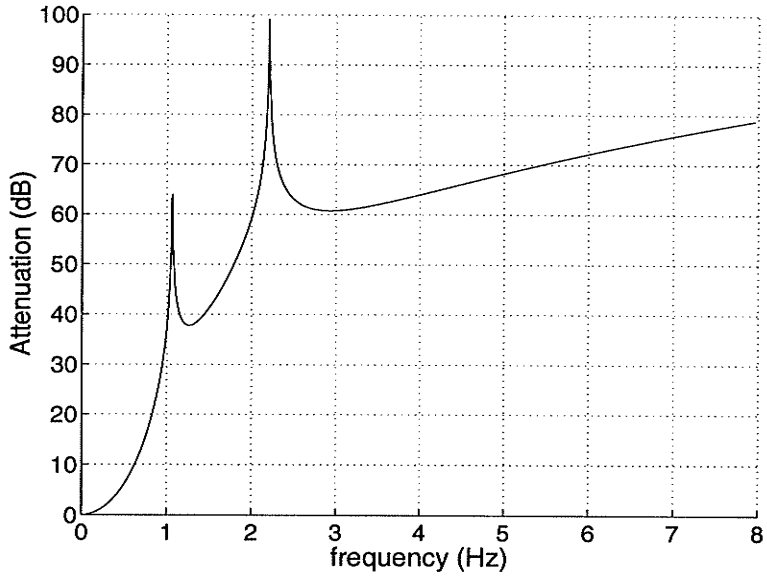

Fig. 5.1 Attenuation response (7th order)

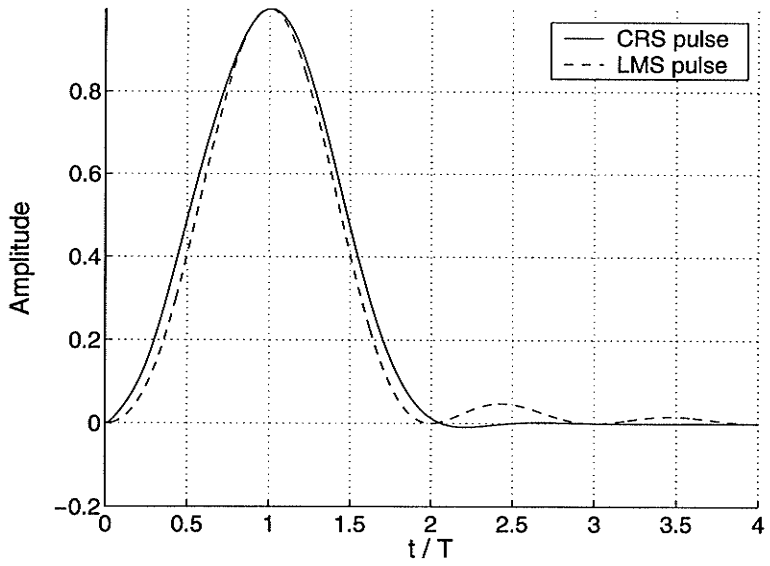

Fig. 5.2 Time response (7th order)

Table 5.2: Zeros and poles of a 7th order linear phase filter

Zeros	Poles
$\pm j\,6.6825$	$-2.6857 \pm j\,5.4207$
$\pm j\,13.8319$	$-4.0701 \pm j\,3.5172$
	$-4.7583 \pm j\,1.7393$
	-4.9718

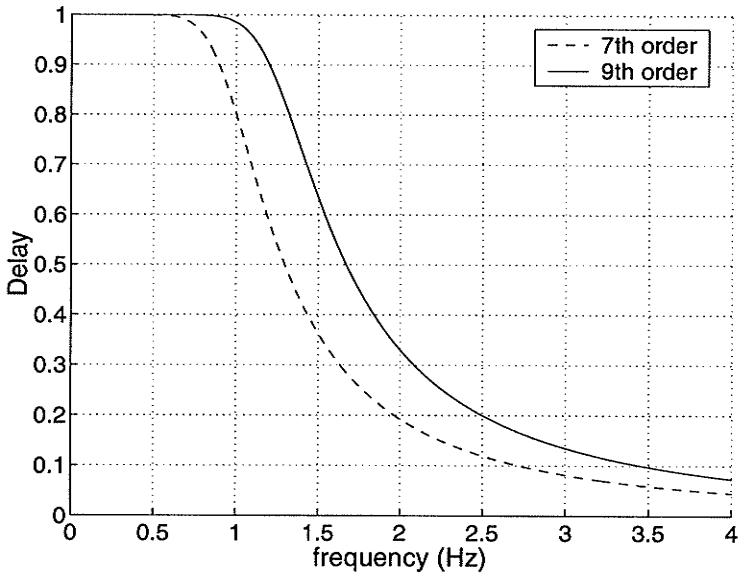

Fig. 5.3 Delay response

Further improvement is possible by allowing more transmission zeros at infinity, an extra pair of transmission zeros is added at infinity by increasing the order n to 9. The improvement is demonstrated through the following two cases:

Case A: Using a 9th degree linear phase polynomial for the denominator and two pairs of finite transmission zeros at $\pm j2\pi$ and $\pm j4\pi$, the position of the second pair is adjusted for reduced pulse amplitude at $t = 2T$ to $\pm j$ 14.7455. The resulting transfer function zeros and poles are as given in Table 5.3 (columns 1, 2), with a constant factor K= 4014.4611. The delay response of the 7th and 9th order filters is shown on Fig. 5.3.The attenuation response and the corresponding pulse are shown in dashed line in Fig. 5.4, and Fig. 5.5, respectively.

Case B: Adjusting the position of both transmission zero pairs, the resulting set is $\pm j$ 6.6825 and $\pm j$ 13.8319, and the constant factor K= 4033.3546. A_s exceeds 30 dB and the corresponding pulse achieves better jitter performance than that of the raised-cosine spectrum pulse and the LMS optimum pulse. The attenuation response is shown in Fig. 5.4, and the corresponding pulse is shown in Fig. 5.5, in solid line. The pole-zero description of this case is given in Table 5.3 (columns 2, 3), and performance of both cases is also summarized in Table 5.4 (columns 3 and 4).

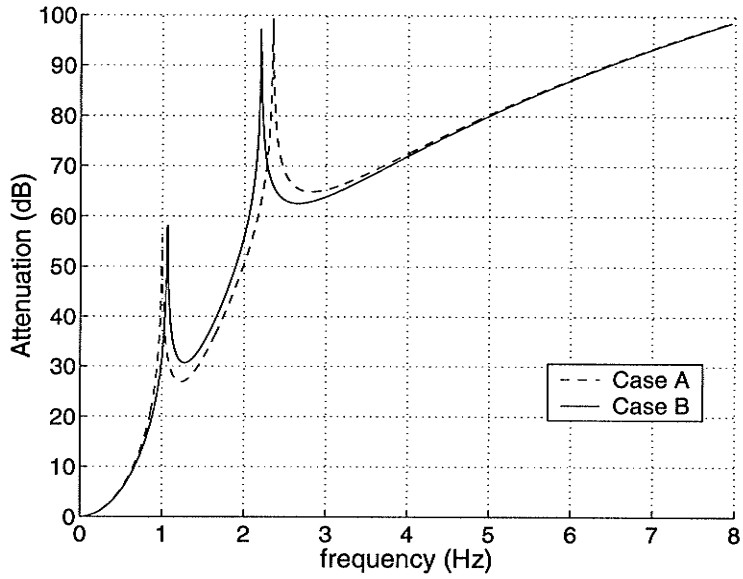

Fig.5.4 Attenuation response (9th order)

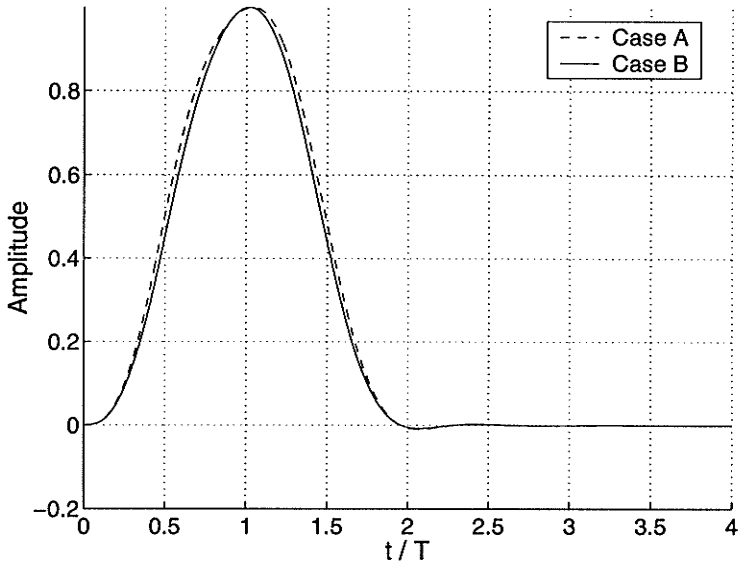

Fig. 5.5 Time response (9th order)

Table 5.3: Zeros and poles of a 9th order linear phase filter

Case A		*Case B*
Zeros	Poles	Zeros
$\pm j\,6.2832$	$-2.9793 \pm j\,7.2915$	$\pm j\,6.6825$
$\pm j\,14.7455$	$-4.6384 \pm j\,5.3173$	$\pm j\,13.8319$
	$-5.6044 \pm j\,3.4982$	
	$-6.1294 \pm j\,1.7378$	
	-6.2970	

Table 5.4: Design examples performance summary

Order n	7	9	
Case		*A*	*B*
Minimum attenuation A_s (dB)	37.6	26.9	30.7
Relative LMS timing error	0.5214	0.2297	0.0760
Relative Jitter performance	0.6210	0.1814	0.1549

Using 100% excess bandwidth indicated by a rolloff factor $\alpha = 1$, the performance of the CRS pulse of Fig. 5.5 (*Case B*) in the presence of jitter is compared to the theoretical performance of the triangular pulse and the raised-cosine pulse spectrum for jitter levels up to 20% of the sampling period T is shown in Fig. 5.6. Since exact mathematical expressions are used to represent the raised-cosine spectrum pulse and the triangular pulse, the upper two curves shown on Fig. 5.6 represent the best possible performance for these two pulses, i.e. lower bounds on the sampling error. Superior performance of the CRS pulse is demonstrated.

A detailed discussion of the use of the triangular function as target for filter design, and jitter performance of the resulting pulse is given in Chapter **3**.

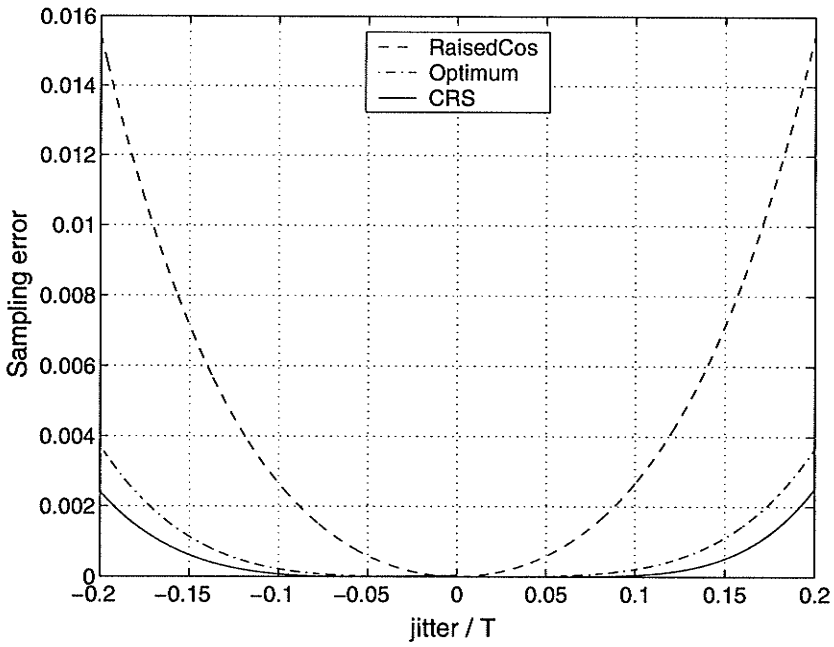

Fig. 5.6 Performance in the presence of jitter

5.4 Pulse Shaping Network

LC networks exhibit low component sensitivity, and ladder networks are used as prototypes for active filters as well as Wave Digital filters [27]. It is therefore useful to realize the transfer function as a ladder LC network, terminated in 1-Ohm resistors.

The driving point admittance is

$$Y = \frac{g-h}{g+h} \tag{5-5}$$

where g and h are the scattering polynomials defined in the Belevitch representation of the network scattering parameters [28]. We have the zeros and poles of the transfer function which determine the scattering polynomials f and g up to a constant. Using the Feldtkeller Equation we can determine h from f and g.

The synthesis algorithm removes sections one at a time to realize the transmission zeros. Partial removal of poles at infinity from the admittance (realizing a shunt capacitance) is required to enable the realization of finite transmission zeros, which are realized first. The partial removal of a pole at infinity from the admittance is done in such a way that the remaining impedance has a pole at one of the transmission zeros. This pole is then realized as a parallel LC section. Once all finite transmission zeros have been realized, the transmission zeros at infinity are removed by alternately removing poles at infinity from the admittance (realizing a capacitance) and from the impedance (realizing an inductance).

The number of reactive elements = $m/2+n$. A complete account of this algorithm can be found in [29]. The scattering polynomials f, g, and h, corresponding to the 9th order pulse shaping network are given in Table 5.5. The corresponding ladder circuit realization is shown in Fig. 5.7.

Table 5.5: Scattering polynomials

f	g	h
4033.3546	1.0000	-1.0000
$\pm j$ 6.6825	-2.9793 $\pm j$ 7.2915	-4.3381 $\pm j$ 5.6169
$\pm j$ 13.8319	-4.6384 $\pm j$ 5.3173	-6.2954 $\pm j$ 4.3598
	-5.6044 $\pm j$ 3.4982	-2.9701 $\pm j$ 7.2658
	-6.1294 $\pm j$ 1.7378	-7.8272 $\pm j$ 1.6394
	-6.2970	-0.0004536

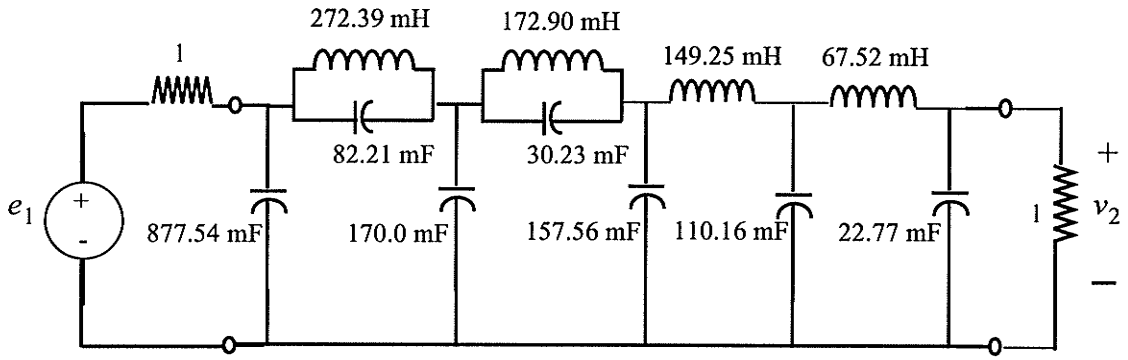

Fig. 5.7 LC ladder realization of a 9th order linear phase transfer function

5.5 Equiripple Attenuation Response for the Linear Phase Design

The transmission zeros can be chosen to give an equiripple attenuation $a(\omega)$ in the stopband [24]. The attenuation is given by

$$a(\omega) = -20\log|H(j\omega)| = -20\left[\log|K| + \sum_{k=1}^{m/2} \log\left|\omega^2 - \omega_k^2\right| - \log|Q_n(j\omega)|\right] \quad (5\text{-}6)$$

$a_o(\omega)$ is specified for the frequency domain in the stopband $\omega_s \le \omega \le \infty$ in the form of a piece-wise linear curve. The initial values of the transmission zeros (attenuation poles) are placed in the stopband, and the minima of $a(\omega) - a_o(\omega)$ are calculated using the initial values of the parameters K and ω_k. Equation(5-6) contains $m/2 + 1$ free parameters. An additional free parameter M can be assigned a fixed value from the attenuation specification in the stopband to be used as reference attenuation level in the stopband. The parameters K and ω_k are to be determined.

To analyze the variation of the attenuation function $a(\omega)$ w.r.t. variation at the minimum points, Equation (5-6) is rewritten using the natural logarithm:

$$a(\omega) = -\frac{20}{\ln(10)}\left[\ln|K| + \sum_{k=1}^{m/2} \ln\left|\omega^2 - \omega_k^2\right| - \ln|Q_n(j\omega)|\right] \quad (5\text{-}7)$$

K in the first term is chosen so that the magnitude of the transfer function is unity at $\omega = 0$; the second term, where complex conjugate values have been paired, is determined by the points of minima; the last term is fixed.

It is required that the attenuation at all minimum points in the stopband satisfy the relation

$$a(\omega_i) + \sum_{k=1}^{m/2} \frac{\partial}{\partial \omega_k} a(\omega_i)\Delta\omega_k = a_o(\omega_i) + M \quad (5\text{-}8)$$

This relation is obtained through linearization of the attenuation at the current approximate value of the parameters ω_k and its variation at the minimum points ω_i of $a(\omega) - a_o(\omega)$. Equation (5-8) expresses the requirement that the approximation of the attenuation function at the minimum points agrees with the specification $a_o(\omega)$, to within an additive constant M.

A total of $m/2 + 1$ linear equations are obtained for the $m/2 + 1$ variables $\Delta\omega_k$ and M. Evaluating the attenuation function at the $m/2$ minimum points ω_i and at the band edge ω_s produces a set of $m/2 + 1$ linear equations $Ax = b$ where

$$A_{ik} = \begin{cases} \dfrac{\partial}{\partial \omega_k} a(\omega)\Big|_{\omega = \omega_i} & i = 1, 2, \ldots, m/2 + 1;\ k = 1, 2, \ldots, m/2 \\ -1 & i = 1, 2, \ldots, m/2 + 1;\ k = m/2 + 1 \end{cases} \tag{5-9}$$

$$\frac{\partial}{\partial \omega_k} a(\omega) = \frac{20}{\ln(10)} \frac{2\omega_k}{\omega^2 - \omega_k^{\,2}}$$

$$b_i = -(a(\omega_i) - a_o(\omega_i)), \quad i = 1, 2, \ldots, m/2 + 1$$

and

$$x_k = \Delta\omega_k, \quad k = 1, 2, \ldots, m/2; \quad x_{m/2+1} = M$$

The new ω_k, $\omega_k' = \omega_k + \Delta\omega_k$.

The linear system of equations is solved, and the determined correction values are added to the corresponding initial values, possibly after multiplication by a positive step size factor <1 so that the norm of $a(\omega) - a_o(\omega)$ does not increase at any step.

Improved values for the approximation parameters are obtained, and thereby an improved attenuation function. This process is repeated until a predetermined tolerance requirement is satisfied. A more general form of this procedure for determining the transmission zeros for equiripple attenuation response can be found in [24].

A transfer function is constructed using a 9th order linear phase polynomial for the denominator and the method described above for selecting the transmission zeros. The resulting transfer function is given in pole-zero form by the zeros and the poles listed in Table 5.6 (columns 1, and 2). For 0 dB at $\omega = 0$, the constant factor is $K = 0.04280$. The resulting attenuation response is shown in Fig. 5.8 (solid line); the dotted line depicts the specification for the attenuation: $A_p = 0.01$ for $f \le 0.9/\pi$, $A_s = 40\ dB$ at $f = f_s = 1$, and $66\ dB$ for $f \ge 4$.

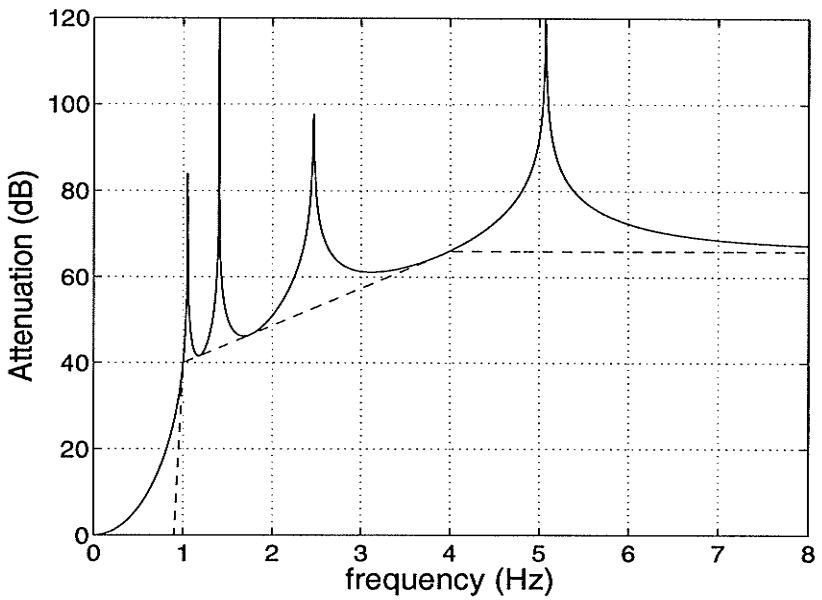

Fig. 5.8 Attenuation response

Table 5.6: Zeros and poles of the equiripple attenuation response design example

Zeros	Poles
$\pm j\,6.5942$	$-2.9793 \pm j\,7.2915$
$\pm j\,8.8067$	$-4.6384 \pm j\,5.3173$
$\pm j\,15.4593$	$-5.6044 \pm j\,3.4982$
$\pm j\,31.6028$	$-6.1294 \pm j\,1.7378$
	-6.2970

5.6 Conclusions

To improve performance in the presence of jitter the sidelobes of the pulse must be attenuated; the linear phase design produces pulses with extremely reduced side lobes so that the pulse energy is essentially packed within the mainlobe.

Performance of the CRS pulse in the presence of jitter is found to be superior to that of the triangular pulse and the raised-cosine pulse, it also outperforms the LMS optimum pulse in some cases, e.g. *Case B* of Sect. **5.3**.

The linear phase design represents an alternative method to generate the Nyquist pulse using realizable filters with purely imaginary transmission zeros enabling filter implementation in terms of ladder LC networks which have low component sensitivity.

It is flexible, intuitive, and robust, it does not suffer any numerical instabilities which some other design methods are vulnerable to.

It was noted in Chapter 3 that the potential jitter performance demonstrated by the ideal triangular pulse in Fig. 3.2 is not achieved by the practical triangular pulse jitter performance as shown in Fig. 3.6. In addition to having superior jitter performance to the raised-cosine pulse, the CRS pulse can be designed to surpass the ideal performance of the triangular pulse and the optimum pulse with a rolloff factor $\alpha = 1$.

Chapter 6

Digital Transmit and Receive Linear Phase Matched Filters

The relation between the causal real symmetric pulse and the linear phase characteristic is formally proved; it is shown that linear phase is necessary and sufficient condition for symmetric unit-sample response. The causal real symmetric pulse treatment which was presented in Chapter 4 in the continuous time domain, is extended here to the discrete time domain and the discrete-time raised-cosine pulse. Real symmetric pulse transmission under a linear phase condition leads to a linear phase pulse shaping filter which is its own match. The transmission zeros of the discrete-time raised-cosine pulse are finite. Consequently the transfer function of the shaping filter is no longer an approximation, but is exactly obtained from the z-transform of the pulse, and the discrete-time delayed raised-cosine is perfectly reconstructed as the unit-sample response of the filter. FIR filters for various values of the delay parameter are described.

6.1 Introduction

The causal real symmetric pulse treatment which was presented in Chapter 4 in the continuous time domain, is extended here to the discrete time domain.
The relation between the causal real symmetric pulse and the linear phase characteristic is formally proven in the discrete time domain; it is shown that linear phase is necessary and sufficient condition for symmetric unit sample response.

The discrete-time delayed raised-cosine pulse is analyzed in Sect. **6.3**. Its frequency response is derived with the delay as a parameter. Unlike the continuous-time raised-cosine pulse, the discrete-time delayed raised-cosine pulse has a finite number of transmission zero pairs and thus can be perfectly reconstructed as the unit-sample response of the filter. The z-transform is also derived leading to an FIR filter design. The digital filter design is discussed in Sect. 6.4 where FIR transfer function examples are given for various orders and delay values.

6.2 Discrete-Time Causal Real Symmetric Unit-Sample Response and Linear Phase

Similar to the discussion of the raised-cosine pulse in the context of matched filter design in Chapter 4, the motivation for considering a discrete-time version of the raised-cosine pulse is based on the fact that if this delayed, discrete-time, and symmetric pulse is generated by the shaping filter at the transmitter, the delayed discrete-time raised-cosine pulse will be matched to a receive filter which is identical to the transmit filter.
Causal real symmetric unit-sample response leads to a receive filter which is identical to the transmit filter (both are digital), and is equivalent to a linear phase response as proved by the following theorem.

THEOREM 6.1:

The real unit-sample response sequence $h[n]$ is symmetric if and only if the phase is linear.

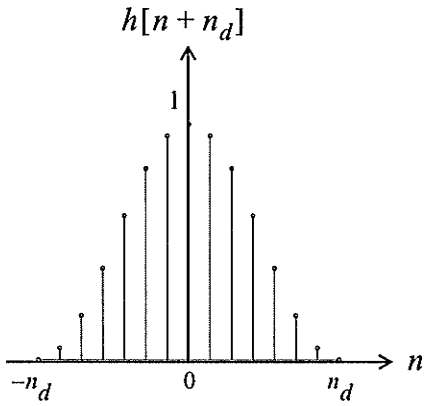

Fig. 6.1a Real symmetric pulse

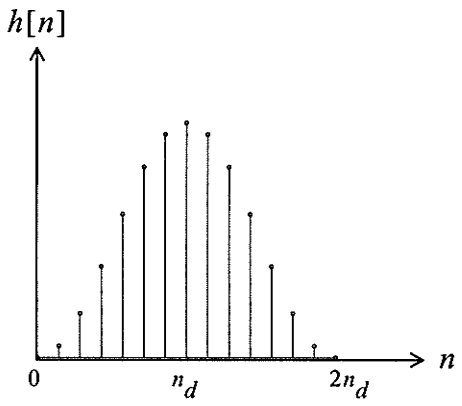

Fig. 6.1b Real delayed symmetric pulse

Proof:

The discrete-time Fourier transform (DTFT) of a real sequence $h[n]$ is [30]

$$H(e^{j\omega}) = \sum_{n=-\infty}^{\infty} h[n]\ e^{-j\omega n}$$

Replacing n by $n + n_d$

$$H(e^{j\omega}) = \sum_{n=-\infty}^{\infty} h[n + n_d]\ e^{-j\omega(n+n_d)}$$

Even symmetry of $h[n]$ about n_d implies $h[n + n_d] = h[-n + n_d]$, it follows that

$$H(e^{j\omega}) = e^{-j\omega n_d} \sum_{n=-\infty}^{\infty} h[-n + n_d]\ e^{-j\omega n}$$

Let $m = -n + n_d$, then

$$H(e^{j\omega}) = e^{-j2\omega n_d} \sum_{n=-\infty}^{\infty} h[m]\ e^{jm\omega}$$

$$H(e^{j\omega}) = e^{-j2\omega n_d} H(e^{-j\omega})$$

$$\angle H(e^{j\omega}) = -2\omega n_d + \angle H(e^{-j\omega})$$

Since $\angle H(e^{-j\omega}) = -\angle H(e^{j\omega})$ for real signals, it follows that

$$\angle H(e^{j\omega}) = -n_d\omega. \qquad (6\text{-}1)$$

Thus, linear phase is necessary for an even symmetric unit-sample response $h[n]$.

To prove the sufficiency condition, assume a linear phase:

$$\angle H(e^{j\omega}) = -n_d\omega,\ n_d > 0,$$

then

$$H(e^{j\omega}) = \left|H(e^{j\omega})\right| \angle H(e^{j\omega}) = \left|H(e^{j\omega})\right| e^{-jn_d\omega}$$

It is required to show that the real unit-sample response $h[n]$ is symmetric, that is

$$h[n + n_d] = h[-n + n_d].$$

The unit-sample response can be expressed in terms of the inverse discrete-time Fourier transform (IDTFT) relation:

$$h[n] = \frac{1}{2\pi}\int_{2\pi} H(e^{j\omega})\ e^{j\omega n}\ d\omega$$

The integrand is periodic with period 2π, and the integration is over an interval of length 2π. Replacing n by $n + n_d$

$$h[n + n_d] = \frac{1}{2\pi}\int_{2\pi} H(e^{j\omega})\ e^{j\omega(n + n_d)}\ d\omega$$

$$= \frac{1}{2\pi}\int_{2\pi} \left|H(e^{j\omega})\right| e^{-j\omega n_d}\ e^{j\omega(n + n_d)}\ d\omega$$

$$= \frac{1}{2\pi}\int_{2\pi} \left|H(e^{j\omega})\right| e^{j\omega n}\ d\omega$$

Since $\left|H(e^{j\omega})\right| = \left|H(e^{-j\omega})\right|$ for real signals, then

$$h[n + n_d] = \frac{1}{2\pi}\int_{2\pi} \left|H(e^{-j\omega})\right| e^{j\omega n}\ d\omega$$

$$= \frac{1}{2\pi}\int_{2\pi} \left|H(e^{-j\omega})\right| e^{j\omega n_d}\ e^{j\omega(n - n_d)} d\omega$$

$$h[n+n_d] = \frac{1}{2\pi}\int_{2\pi} H(e^{-j\omega})\ e^{j\omega(n-n_d)}d\omega$$

and replacing ω by $-\omega$

$$h[n+n_d] = \frac{1}{2\pi}\int_{2\pi} H(e^{j\omega})\ e^{j\omega(-n+n_d)}d\omega = h[-n+n_d]$$

Thus it is proven that $h[n]$ is symmetric about n_d, and therefore linear phase is necessary and sufficient for the unit-sample response $h[n]$ to be symmetric. □

6.3 The Discrete-Time Raised-cosine Pulse

Sampling the time-domain raised-cosine pulse (4-3) is achieved by replacing t by nT_s and t_d by n_dT_s, where T_s is the sampling interval.

The discrete time-domain raised-cosine pulse is given by

$$p_{rc}[n] = \begin{cases} \frac{1}{2}(1+\cos(\pi n/n_d)) & |n| \le n_d \\ 0 & otherwise \end{cases} \qquad (6\text{-}2)$$

where n_d is the point of even symmetry, or discrete delay of the discrete-time pulse.

This pulse is shown in Fig. 6.1a with $p_{rc}[n] = h[n+n_d]$, and will be referred to as the discrete-time raised-cosine pulse.

If delayed by n_d, this pulse has even symmetry about n_d and is contained within the main lobe $[0,\ 2n_d]$, as shown in Fig. 6.1b, thus by *Theorem 6.1*, this delayed version has a linear phase or equivalently a constant delay n_d.

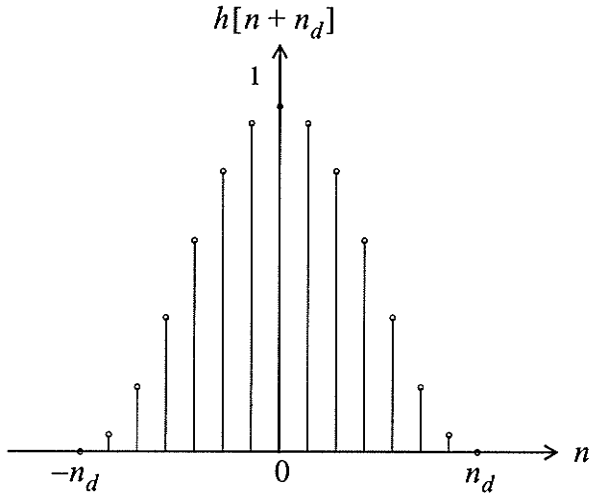

Fig. 6.2 The discrete-time raised-cosine pulse

The spectrum corresponding to the discrete-time raised-cosine pulse with unity maximum amplitude can be obtained from the DTFT as

$$P_{rc}(f) = \frac{1}{2}\frac{\sin(\omega m_d)}{\sin(\omega/2)} + \frac{1}{4}\frac{\sin(\omega - \pi/n_d)m_d}{\sin(\omega/2 - \pi/2n_d)} + \frac{1}{4}\frac{\sin(\omega + \pi/n_d)m_d}{\sin(\omega/2 + \pi/2n_d)} \qquad (6\text{-}3)$$

where $\omega = 2\pi f$, $m_d = n_d + 1/2$, n_d is the discrete delay, and the number of samples per pulse is $2n_d + 1$, which includes two zero samples. The frequency domain representation of the discrete-time raised-cosine pulse given by (6-3) with $n_d = 4$ has infinite attenuation at fractional multiples of π starting at $\pi/2$, specifically at $f = 0.25,\ 0.375,\ 0.5$ as indicated by Fig. 6.3 which shows the ideal attenuation response of the discrete-time

raised-cosine pulse (with 8 samples/pulse) versus frequency f. Equivalently, the transmission zero pairs are $\omega = \pm j\pi/2,\ \pm j3\pi/4,\ \pm j\pi$, for $n_d = 4$.

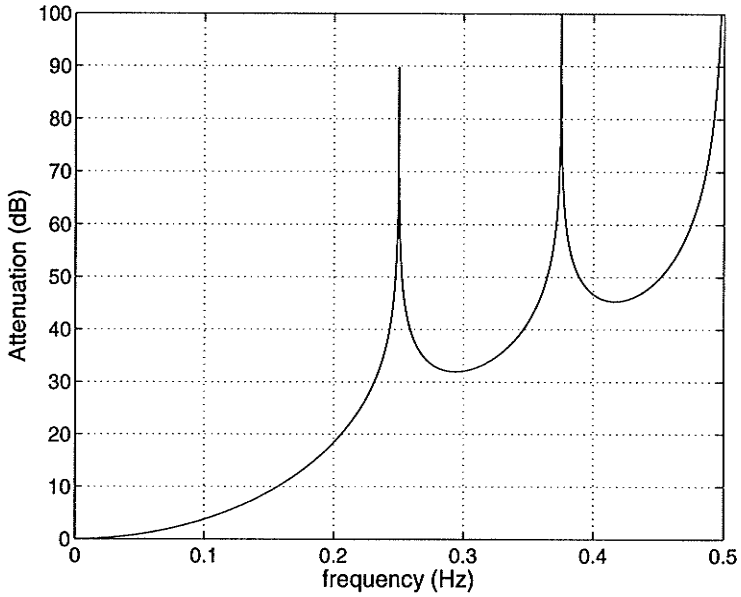

Fig. 6.3 Attenuation response of the ideal discrete-time raised-cosine pulse, $n_d = 4$

Further investigation of the spectrum in (6-3), with respect to the parameter n_d reveals the following relation for the positions of the zeros:

$$f = k/2n_d, \quad k = 2,3,\ldots,n_d \tag{6-4}$$

The highest zero is always at $f = 0.5$, of which there is a pair.

Unlike the analog case where the number of transmission zeros is infinite, the spectrum of the discrete-time raised-cosine pulse has only a finite number of transmission zeros. Therefore it can be exactly reconstructed.

The raised-cosine pulse given by (6-2) when delayed by n_d becomes

$$p_{n_d}[n] = \frac{1}{2}(1 - \cos(\pi n/n_d)), \quad 0 \le n \le 2n_d \tag{6-5}$$

The corresponding z-transform can be obtained as follows:

$$Z\{p_{n_d}[n]\} = P_{n_d}[z] = \sum_{n=-\infty}^{\infty} p_{n_d}[n]\ z^{-n}$$

$$Z\{p_{n_d}[n]\} = \sum_{n=0}^{2n_d} \frac{1}{2}(1 - \cos(\pi n/n_d))\ z^{-n} \tag{6-6}$$

$$Z\{p_{n_d}[n]\} = \sum_{n=0}^{2n_d} \frac{1}{2}(z^{-1})^n - \frac{1}{4}(z^{-1}e^{j\pi/n_d})^n - \frac{1}{4}(z^{-1}e^{-j\pi/n_d})^n$$

$$Z\{p_{n_d}[n]\} = \frac{1}{2}\frac{1-(z^{-1})^{2n_d+1}}{1-z^{-1}} - \frac{1}{4}\frac{1-(z^{-1}e^{j\pi/n_d})^{2n_d+1}}{1-z^{-1}e^{j\pi/n_d}} - \frac{1}{4}\frac{1-(z^{-1}e^{-j\pi/n_d})^{2n_d+1}}{1-z^{-1}e^{-j\pi/n_d}}$$

Manipulating the above, the following expression can be obtained:

$$Z\{p_{n_d}[n]\} = \frac{1}{2}\left(1 - \cos\left(\frac{\pi}{n_d}\right)\right)\frac{z^{2n_d+1} + z^{2n_d} - z - 1}{z^{2n_d-1}(z-1)(z^2 - 2z\cos(\pi/n_d) + 1)} \tag{6-7}$$

The sequence given in (6-6), has zero terms at $n = 0$, and $n = 2n_d$ indicating a highest degree of $2n_d - 1$ for the z-transform. The last two factors in the denominator of (6-7), $(z-1)(z^2 - 2z\cos(\pi/n_d) + 1)$, cancel with equal factors from the numerator such that the denominator is just z^{2n_d-1}; i.e., there are $2n_d - 1$ poles at the origin, consequently the delay is flat at all frequencies.

In particular, the middle term in the last parenthesis in the denominator of (6-7) vanishes when $n_d = 2$, and further simplification reduces the z-transform expression to

$$Z\{p_2[n]\} = \frac{1}{2}(z+1)^2/z^3$$

There are 3 poles at the origin, and 2 zeros on the unit circle at -1, indicating transmission zero pairs at $\pm j\pi$ and this case is of no interest.

Using $n_d = 3$, the ideal spectrum of (6-3) has zeros at $f = 1/3, 1/2$, simplifying (6-7), the z-transform is given by

$$Z\{p_3[n]\} = \frac{1}{4}\frac{(z+1)^2(z^2+z+1)}{z^5}$$

which has 4 zeros on the unit circle: 2 at -1, $\frac{1}{2}(-1 \pm j\sqrt{3})$, and 5 poles at the origin resulting in a flat delay response of 3.

From the above discussion, it can be seen that a $(z+1)^2$ factor is part of the numerator in each case. Also, the denominator of the z-transform (6-7) can be reduced to z^{2n_d-1} in every case. It is of interest to find an expression for the z-transform without the factors that cancel out: the $(z-1)$ and the $(z^2 - 2z\cos(\pi/n_d) + 1)$ factors. So a single zero at 1 and a pair of zeros at $e^{\pm j\pi/n_d} = \cos(\pi/n_d) \pm j\sqrt{1-(\cos(\pi/n_d))^2}$ must be removed from the denominator. It is straight forward to verify that $(z-1)$, and $(z^2 - 2z\cos(\pi/n_d) + 1)$ are factors of the numerator polynomial. To do so, start with the numerator polynomial given by (6-7) as

$$N(z) = z^{2n_d+1} + z^{2n_d} - z - 1 \qquad (6\text{-}8)$$

Evaluating $N(z)$ at $z = 1$, and $z = e^{\pm j\pi/n_d}$ produces zero value in each case.

Moreover, $N(z)$ and $\frac{d}{dz}N(z)$ both evaluate to zero at -1 indicating a double zero at -1, so $(z+1)^2$ is a factor of the $N(z)$ (but not of the denominator).

It is convenient to express the z-transform without these common factors, which can be achieved by starting with the original sequence. Rewriting (6-6) according to (6-7), and cancelling out the common factors, the z-transform of the delayed raised-cosine pulse of (6-5) can be written as:

$$Z\{p_{n_d}[n]\} = \frac{1}{2}\frac{\sum_{k=1}^{2n_d-1}(1-\cos(k\pi/n_d))\ z^{2n_d-1-k}}{z^{2n_d-1}} \tag{6-9}$$

It is useful to have the z-transform expressed in a product of factors form, which can be done using the zeros given in (6-4) and listed in Table 6.1.

The number of zeros and their positions is a function of the delay parameter n_d. However, as shown above, there is always a pair of zeros at $z = -1$ for any value of n_d, which corresponds to the transmission zero at $\omega = \pi$.

$$Z\{p_{n_d}[n]\} = K_z\frac{(z+1)^2\prod_{k=2}^{n_d-1}(z-e^{\pm jk\pi/n_d})}{z^{2n_d-1}} \tag{6-10}$$

where the constant factor $K_z = \frac{1}{2}(1-\cos(\pi/n_d))$.

6.4 The Digital Filter Design

The transfer function of a filter of order n in the z-domain can be written as

$$H(z) = \frac{P_m(z)}{Q_n(z)} = K_z z^{n-m} \prod_{k=1}^{m} (z - z_k) / \prod_{k=1}^{n} (z - p_k), \quad K_z \neq 0 \tag{6-11}$$

where m is the degree of the numerator polynomial, n is the degree of the denominator polynomial, and $z = e^{sT_s}$, the z_k are the zeros and the p_k are the poles of the filter.

Specifically, from (6-10), the transfer function of the filter can be expressed as

$$H(z) = K_z \frac{(z+1)^2 \prod_{k=2}^{n_d - 1} (z - e^{\pm jk\pi/n_d})}{z^{2n_d - 1}} \tag{6-12}$$

where the constant factor K_z is as defined for (6-10).

There are $2n_d - 2$ zeros on the unit circle, these are equivalent to $j\omega$-axis transmission zeros which produce maximum attenuation, and there are $2n_d - 1$ poles at the origin which result in a flat attenuation at all frequencies. The order of the filter is $2n_d - 1$.

(6-12) can be written in terms of the unit delay z^{-1} as:

$$H(z) = K_z z^{-1} \prod_{k=2}^{n_d} (1 - e^{\pm jk\pi/n_d} z^{-1}) \tag{6-13}$$

The minimum number of samples per pulse which can be used without appreciable SNR degradation at the detector is determined to be 8, which is also considered to be a good compromise between good performance and low implementation complexity [31, 32].

Substituting $n_d = 4$ in (6-7) and simplifying, the transfer function is given by

$$H(z) = \frac{1}{2}(1 - 1/\sqrt{2})\frac{(z+1)^2(z^2+1)(z^2+\sqrt{2}z+1)}{z^7} \tag{6-14}$$

There are 6 zeros on the unit circle: 2 at -1, and 4 at $\pm j$, $\frac{1}{\sqrt{2}}(-1 \pm j)$, and 7 poles at the origin, as shown in Fig. 6.4.

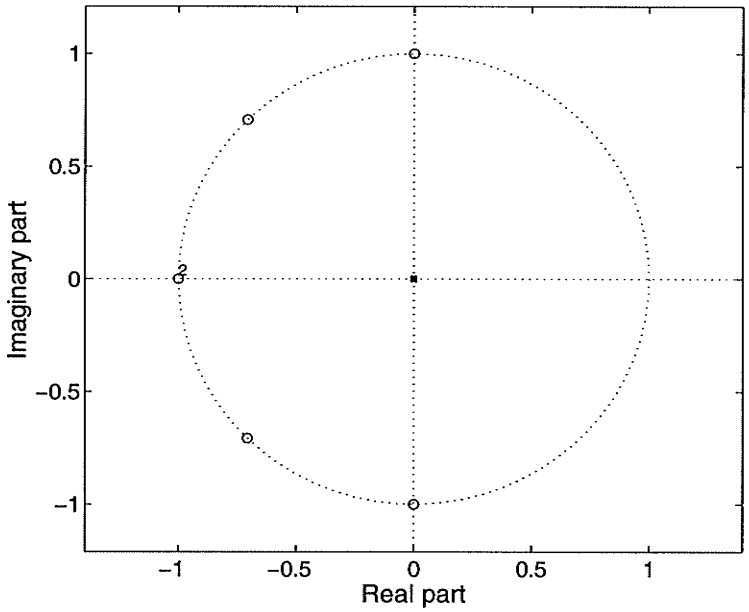

Fig. 6.4 Zeros and poles in the z-plane for the ideal discrete-time raised-cosine pulse, $n_d = 4$

The causal real symmetric pulse is generated as the unit-sample response of the linear phase FIR filter. In general, the output of such a system can be expressed as:

$$\begin{aligned} Y(z) &= H(z)X(z) \\ &= \left(\sum_{n=0}^{N-1} h[n]\ z^{-n} \right) X(z) \\ &= \sum_{n=0}^{N-1} h[n](z^{-n}X(z)) \end{aligned}$$

taking the inverse transform of both sides

$$y[n] = \sum_{m=0}^{N-1} h[m]\ x[n-m] \tag{6-15}$$

FIR filters can be implemented in a variety of alternative forms, which are theoretically equivalent [33]. The direct-form realization follows directly from the convolutional sum relationship (6-15), and corresponds to the most straight forward ordering of the additions and multiplications implied by (6-15). Fig. 6.5 shows the signal flow graph for direct-form implementation of the linear phase filter with $n_d = 4$. The filter coefficients, which can be obtained from (6-9), are as follows

$$\begin{aligned} h[1] = h[7] = (2-\sqrt{2})/4, \quad h[2] = h[6] = 1/2 \\ h[3] = h[5] = (2+\sqrt{2})/4, \quad h[4] = 1 \end{aligned}$$

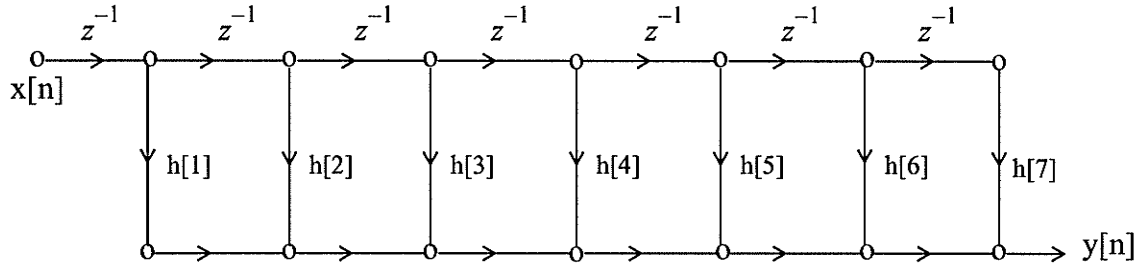

Fig. 6.5 Signal flow graph for an FIR filter

The z-transform poles and zeros in each case are listed in Table 6.1, along with other cases. As can be seen from Table 6.1, the higher the number of samples used, the higher is the order of the filter and the narrower is the passband; the delay also increases with increased number of samples. For example, to have the lowest pair of transmission zeros at $f = 0.1$ Hz, the number of samples must be 20, leading to a filter order of 19. The associated delay is 10 as listed on the last row of Table 6.1.

Table 6.1: Transfer function examples

Delay	Transmission zeros (Hz)	z-domain		
		K_z	Zeros	No. of poles
2	$1/2$	0.5000	$-1, -1$	3
3	$1/3,\ 1/2$	0.2500	$-e^{\pm j2\pi/3}, -1, -1$	5
4	$1/4,\ 3/8,\ 1/2$	0.14645	$\pm j, -e^{\pm j3\pi/4}, -1, -1$	7
5	$\frac{1}{5}, \frac{3}{10}, \frac{2}{5}, \frac{1}{2}$	0.09549	$e^{\pm j0.4\pi}, e^{\pm j0.6\pi}, e^{\pm j0.8\pi}, -1, -1$	9
8	$\frac{1}{8}, \frac{3}{16}, \frac{2}{8}, \frac{5}{16}, \frac{3}{8}, \frac{7}{16}, \frac{1}{2}$	0.03806	$e^{\pm j0.25\pi}, e^{\pm j0.375\pi}, \pm j, e^{\pm j0.626\pi}, e^{\pm j0.75\pi}, e^{\pm j0.875\pi}, -1, -1$	15
10	$\frac{1}{10}, \frac{3}{20}, \frac{2}{10}, \frac{5}{20}, \frac{3}{10}, \frac{7}{20}, \frac{4}{10}, \frac{9}{20}, \frac{1}{2}$	0.02447	$e^{\pm j0.2\pi}, e^{\pm j0.3\pi}, e^{\pm j0.4\pi}, \pm j, e^{\pm j0.6\pi}, e^{\pm j0.7\pi}, e^{\pm j0.8\pi}, e^{\pm j0.9\pi}, -1, -1$	19

The number of non-zero samples of the unit-sample response is always odd and equals the number of poles, which is greater than the number of zeros by 1.

There is a pair of the highest transmission zeros at $f = 0.5$, and all poles are at the origin.

The unit-sample response width, or duration is twice the delay n_d and is greater than the number of non-zero samples by 1 because of the existence of a zero sample at the origin and at the end point $2n_d$ in every case. The length of the filter is twice the delay.

6.5 Conclusions

The development of the digital version of the matched filter is similar to that of the continuous-time version of Chapter 4. However, unlike the analog case where the number of transmission zero pairs is infinite and the transfer function is an approximation, the spectrum of the discrete-time raised-cosine pulse has only a finite number of transmission zeros and therefore it can be represented exactly by a transfer function which is simply the z-transform of the pulse. The discrete-time raised-cosine is perfectly reconstructed as the unit-sample response of the filter. FIR filters for various values of the delay parameter are described, and a network realization example is given.

Conclusions

The objective set out for this work (as stated in Sect. 1.2) includes the following:

1- To design a method for generating a Nyquist pulse with better jitter performance than the standard raised-cosine pulse, while achieving maximum attenuation in the stopband using the least filter order n.

2- To investigate the relation between pulse symmetry and the phase characteristic and use it to design a transmit and receive matched filter pair.

Having zero derivatives at the sampling instants, the triangular function has been shown to have better performance in the presence of jitter than the raised-cosine function. The impulse response of an 8th order filter, which is designed using the triangular function as a target is shown to outperform the raised-cosine target function, and hence outperforms the filter designed with the raised-cosine function as a target. The triangular pulse has better performance than the raised-cosine spectrum pulse under the worst-case design criterion, as well as under the LMS design. However, the design method does not produce a close fit, consequently, the performance of the ideal triangular pulse in the presence of jitter could not be achieved by the time response of the designed filter. Better approximation could be achieved with higher order filters. However, this design method suffers from possible result inaccuracy as the transfer function polynomials are in coefficient form, and the matrix representing the set of linear equations tends to becomes ill conditioned and close to singular. Both spectra used in conjunction with the worst-case and the least-mean-square method imply an infinite attenuation for the entire stopband which can not be achieved with practical filters. Hence, the triangular rolloff spectrum and the spectrum

corresponding to the optimum pulse are theoretical results that cannot be exactly produced in practice as practical filters do not have infinite attenuation over the entire stopband. The filter necessarily cannot be strictly bandlimited.

Assuming communication through a linear channel with AWGN, the receive filter which is matched to the signal maximizes the output signal–to–noise ratio. The pulse shaping is split between the transmitter and the receiver. With the second point of the design objective in mind, causal real symmetric impulse response and linear phase are discussed and it is shown that if a causal real symmetric pulse is transmitted through the linear Gaussian channel, it will be matched to a receive filter which is identical to the transmit filter. Linear phase is necessary and sufficient for the real impulse response to be symmetric, and proof is given in the continuous-time and the discrete-time domains.
The time-domain delayed raised-cosine pulse is considered for a Nyquist pulse design, its ideal spectrum is analysed and the transmission zeros are determined.

A rational function approximation to the spectrum of the delayed raised-cosine pulse is required. A good approximation to the causal symmetric raised-cosine pulse is provided by the impulse response of an approximately linear phase filter. The denominator of the transfer function of the filter is a linear phase polynomial generated by a recurrence relation. A formula to generate the linear phase polynomial in coefficient form is also available. The numerator polynomial includes the first two transmission zero pairs corresponding to the raised-cosine pulse, which are on the $j\omega$-axis, and the lowest filter

order was determined to be 7. The generated pulse is essentially contained within the main lobe as required for improved jitter performance.

The combination of even symmetry of time response, and conjugate transmission zero pairs leads to a linear phase pulse shaping filter which is its own match. It can perform both tasks of transmit and receive filter, which can be advantageous in situations where the transmitter and receiver are at the same physical location.

Two identical 9th order filters are used as a transmit and receive matched filter pair. Frequency scaling is used to generate a Nyquist pulse which is half as wide as the nominal pulse, so that the received pulse, which will be twice as wide as the transmit pulse, and the sampling period at the receiver is unity. The cascade of the transmit filter and the receive filter achieve a minimum stopband attenuation of 66 dB. Due to pulse symmetry, the output pulse of the receive filter is the convolution of the transmit pulse by itself, consequently its shape is narrower and its amplitude near the end points is smaller than that of the transmit pulse, which improves the jitter performance considerably.

Performance of the receive pulse in the presence of jitter is quite satisfactory, and the sampling error is virtually zero.

The causal real symmetric Nyquist pulse design is discussed further and performance of the CRS pulse in the presence of jitter is found to be superior to that of the triangular pulse and the raised-cosine spectrum pulse with a rolloff factor $\alpha = 1$; it also outperforms the LMS optimum pulse in some cases, e.g. *Case B* of Sect. **5.3**. The linear phase design represents an alternative method to generate the Nyquist pulse using realizable fil-

ters with purely imaginary transmission zeros enabling filter implementation in terms of ladder LC networks which have low component sensitivity. The design method is flexible and robust, it does not suffer any numerical instabilities which some other design methods are vulnerable to.

The causal real symmetric pulse method is extended to the discrete time domain and the discrete-time raised-cosine pulse. The development of the digital version of the matched filter is similar to that of the continuous-time version of Chapter 4. However, unlike the continuous-time case where the number of transmission zero pairs is infinite, the spectrum of the discrete-time raised-cosine pulse has only a finite number of transmission zeros. Therefore it can be represented exactly by a transfer function which is simply the z-transform of the pulse. The discrete-time raised-cosine is perfectly reconstructed as the unit-sample response of the filter. FIR filters for various values of the delay parameter are described. The objective of this work is achieved with good results.

REFERENCES

[1] H. Nyquist, "Certain Topics in Telegraph Transmission Theory," *AIEE Trans.*, vol. 47, pp. 617-644, Feb. 1928.

[2] N. C. Beaulieu, "Introduction to 'Certain Topics in Telegraph Transmission Theory'," *Proceedings of the IEEE*, vol. 90, No. 2, February 2002.

[3] R. A. Gibby and J. W. Smith, "Some Extensions of the Nyquist's Telegraph Transmission Theory," *Bell Syst. Tech. J.*, vol 44, pp.1487-1510, Sept. 1965.

[4] D. A. Spaulding, "Synthesis of Pulse-Shaping Networks in the Time Domain," *Bell Syst. Tech. J.,* vol 48, pp.2425-2444, Sept. 1969.

[5] S. E. Nader, and L. F. Lind, "Optimal Data Transmission Filters," *IEEE Trans. Circuits Syst.*, vol. CAS 26, No. 1, pp 36-45, Jan. 1997.

[6] H.Baher, and J. Beneat, "Design of Analog and Digital Data Transmission Filters", *IEEE Trans. Circuits Syst.*, vol. 40, No.7, July 1993.

[7] Xiang-Gen Xia, "A Family of Pulse Shaping Filters with ISI-Free Matched and Unmatched Filter Properties," *IEEE Trans. On Comm.* vol.45, No. 10, October 1997.

[8] N. Algha and P. Kabal, "Generalized Raised-Cosine Filters," *IEEE Trans. Comm.*, vol. 47, No. 7, July. 1999.

[9] J. O. Scanlan "Pulses Satisfying The Nyquist Criterion," *Electronics Letters,* vol 28 (1), pp. 50-52, January 1992.

[10] L. E. Franks "Further results on Nyquist's problem in pulse transmission,", *IEEE Trans.on Comm.* vol 16 (2), pp. 337-340, April 1968.

[11] S. Mneina, and G. O. Martens "Analysis of Timing Sensitivity and Nyquist Pulse Design," *Electrical and Computer Engineering, 2002.IEEE CCECE 2002.Canadian Con-*

ference on, vol.2, May, 2002, pp. 1059 -1063.

[12] J. Proakis and M. Salehi, *Communication Systems Engineering*. Prentice Hall, 1994.

[13] I. S. Gradshteyn and I. M. Ryzhik, *Tables of integrals, series, and products*. Academic Press,1980.

[14] R. Courant and D. Hilbert, *Methods of mathematical physics.* Interscience Publishers, New York, 1953.

[15] Mneina, S. "Linear Phase Data Transmission Filters," *Proc. GradCon'98*, The University of Manitoba, May 1998. http://www.ee.umanitoba.ca/~gradcon/gradcon98/proceedings.

[16] S. Mneina, and G. O. Martens "Filter design targets with reduced jitter effect," *in Proc. PACRIM2001 IEEE Pacific Rim Conference on Communications, Computers and Signal Processing, vol. 1*, August, 2001, pp. 172-175.

[17] E.E.Hassan, and H. Ragheb, "Design of Linear Phase Nyquist Filters," *IEE Proc. Circuit Devices Syst.*, vol 143 No.3, June 1996.

[18] J. Rhodes, *Theory of Electrical Filters*. Wiley, New York, 1976.

[19] D. O. North "An Analysis of the factors which determines signal/noise discrimination in pulsed carrier systems," *Proceedings of the IEEE*, vol. 51, pp.1016-1027, 1963.

[20] G. L. Turin "An Introduction to Matched Filters," *IEEE Transactions on Information Theory*, vol. IT-6, pp 311-329, 1960.

[21] A.P.R. Opperman and L.P. Lind, "Design Considerations and Applications of Asymmertically Matched Nyquist Low Pass Filters," *IEEE COMSIG 1991Proceedings*, South African Symposium on Communications and Signal Processing, pp 166-71.

[22] J. G. Proakis, *Digital Communications*. New York: McGraw-Hill, 1989.

[23] H. Meyr, M. Moeneclaey and S. A. Fetchel, *Digital Communication Receivers: Synchronization, channel Estimation, and Signal Processing*, Wiley, 1998.

[24] R. Unbehauen, *Netzwerk-und Filter-Synthese*, Oldenbourg Verlag, Muenchen Wein 1993, pp 685-688.

[25] L. Kendall Su, *Time-Domain Synthesis of Linear Networks*, Prentice-Hall, 1971.

[26] S. Mneina, and G. O. Martens "Maximally Flat Delay Pulse Shaping Network," in *Proc.Electrical and Computer Engineering, IEEE CCECE 2002.Canadian Conference on, vol.2*, May, 2002, pp. 1026-1030.

[27] A. Fettweis "Wave Digital Filters: Theory and Design," Proceedings of the IEEE, vol. 74, No. 2, Feb. 1986, pp 270-327.

[28] V. Belevitch, *Classical network theory*, San Francisco, Holden-Day, 1968.

[29] G. O. Martens, *Electric Filter Design Course Notes*, Department of Electrical and Computer Engineering, University of Manitoba, 2003.

[30] R. A. Gabel, R. A. Roberts, *Signals and Linear Systems*. Wiley, 1987.

[31] M. K. Simon "On the Selection of a Sampling Filter bandwidth for a Digital Data Detector," *IEEE Transactions on Communications*, Vol. 20, June 1972, pp. 438-441.

[32] A. Casini, G. Castellini, P. Emiliani "Sampling Rate Selection for a Digital Matched Filter," *Proceedings of the IEEE*, May 1972, pp 112-114.

[33] A. V. Oppenheim, R. W. Schafer, *Digital Signal Processing*. Prentice-Hall, 1975, pp. 155-157.

A1. Derivation of the Worst-Case Design Nyquist Pulse

$$p(t) = 2\int_0^{\infty} P(f)\cos(2\pi ft)df = \int_0^{f_2} [1 + G(f)]\cos(2\pi ft)df$$

$$p(t) = \int_0^{f_2} \cos(2\pi ft)df + \int_0^{f_1} \cos(2\pi ft)df + \int_{f_1}^{f_2} G(f)\cos(2\pi ft)df$$

$$p(t) = \frac{\sin(2\pi ft)}{2\pi t}\Big|_0^{f_2} + \frac{\sin(2\pi ft)}{2\pi t}\Big|_0^{f_1} + \int_{f_1}^{f_2} G(f)\cos(2\pi ft)df$$

$f_1 = (1-\alpha)f_s/2$, $f_2 = (1+\alpha)f_s/2$, $f_s = 1/T$ is the sampling frequency, T is the sampling period, and α is the rolloff factor.

$$p(t) = \frac{1}{\pi t}\sin(\pi f_s t)\cos(\alpha\pi f_s t) + \int_{f_1}^{f_2} G(f)\cos(2\pi ft)df$$

let $x = f - f_s/2$, then $f = x + f_s/2$

$$\int_{f_1}^{f_2} G(f)\cos(2\pi ft)df = \int_{-\alpha f_s/2}^{\alpha f_s/2} G(x + f_s/2)\cos(2\pi(x + f_s/2)t)dx$$

factorising the cosine integrand term into even and odd functions:

$$\cos 2\pi(x + f_s/2)t = \cos(2\pi xt)\cos(\pi f_s t) - \sin(2\pi xt)\sin(\pi f_s t)$$

$$\int_{f_1}^{f_2} G(f)\cos(2\pi ft)df = -\int_{-\alpha f_s/2}^{\alpha f_s/2} G(x + f_s/2)\sin(2\pi xt)\sin(\pi f_s t)dx$$

let $Q(x) = G(x + f_s/2)$, $|f| \le \alpha f_s/2$, and note that $G(f + f_s/2)$ is odd, so $Q(f)$ must be an odd function satisfying $Q(0) = 0$, $Q(\alpha f_s/2) = -1$.

$$\int_{f_1}^{f_2} G(f)\cos(2\pi ft)df = -2\sin(\pi f_s t)\int_0^{\alpha f_s/2} Q(x)\sin(2\pi xt)dx$$

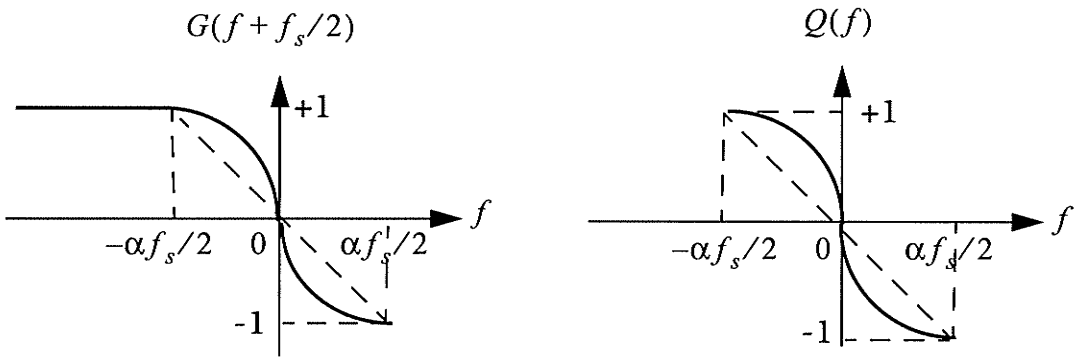

Integrating by parts:

$$\int_{-\alpha f_s/2}^{\alpha f_s/2} Q(x)\sin(2\pi xt)dx = -\frac{Q(x)\cos(2\pi xt)}{2\pi t}\Big|_0^{\alpha f_s/2} + \int_{-\alpha f_s/2}^{\alpha f_s/2} Q'(x)\cos(2\pi xt)dx$$

$$= \frac{\cos(\pi\alpha f_s t)}{2\pi t} + \int_0^{\alpha f_s/2} Q'(x)\cos(2\pi xt)dx$$

$$p(t) = -\frac{1}{\pi t}\sin(\pi f_s t)\int_0^{\alpha f_s/2} Q'(x)\cos(2\pi xt)dx$$

Let $\phi(x) = -Q'(x)$, then $\phi(x)$ is even and

$$\int_0^{\alpha f_s/2} \phi(x)dx = -Q(x)\Big|_0^{\alpha f_s/2} = -(-1-0) = 1$$

$$p(t) = \frac{1}{\pi t}\sin(\pi f_s t)\int_0^{\alpha f_s/2} \phi(f)\cos(2\pi ft)df \qquad (2\text{-}6)$$

$$= \frac{1}{\pi t}\sin(\pi f_s t)\ g(t)$$

$$\text{where } g(t) = \int_0^{\alpha f_s/2} \phi(f)\cos(2\pi ft)df \qquad (2\text{-}7)$$

$g(t)$ is the inverse transform of $\phi(f)/2$.

A2. Derivation of the Intersymbol Interference (ISI)

The interfering signal for detection at $t = 0$ is represented by the pulse train

$$x(t) = \sum_{\substack{n = -\infty \\ n \neq 0}}^{\infty} a_n p(t - nT)$$

so

$$\frac{d}{dt}x(t) = \sum_{\substack{n = -\infty \\ n \neq 0}}^{\infty} a_n \frac{d}{dt}p(t - nT)$$

from (2-6)

$$p(t) = \frac{\sin(\omega_s t/2)}{\pi t} g(t) = \frac{1}{T} Sa(\omega_s t/2) g(t)$$

where $Sa(x) = \frac{\sin(x)}{x}$, $\omega_s = \frac{2\pi}{T}$, and

$$g(t) = \int_0^{\alpha f_s/2} \phi(f) \cos(2\pi f t) df$$

$\phi(f)$ is an arbitrary real even function of f which is band-limited to $\pm\alpha f_s/2$ such that

$$\int_0^{\alpha f_s/2} \phi(f) df = 1 .$$

$$\frac{d}{dt}p(t - nT) = Sa\left(\frac{\pi}{T}(t - nT)\right)\frac{\frac{d}{dt}g(t - nT)}{T} + \frac{g(t - nT)}{T}\frac{d}{dt}Sa\left(\frac{\pi}{T}(t - nT)\right)$$

$$T\frac{d}{dt}p(t-nT)\Big|_{\substack{t=0\\ n\neq 0}} = \frac{g(t-nT)}{T}\frac{d}{dt}Sa\left(\frac{\pi}{T}(t-nT)\right)\Big|_{\substack{t=0\\ n\neq 0}}$$

where $Sa\left(\frac{\pi}{T}(t-nT)\right)\Big|_{\substack{t=0\\ n\neq 0}} = 0$

$$\frac{d}{dt}Sa\left(\frac{\pi}{T}(t-nT)\right) = \frac{d}{dt}\frac{\sin\frac{\pi}{T}(t-nT)}{\frac{\pi}{T}(t-nT)} = \frac{\left(\frac{\pi}{T}\right)^2(t-nT)\cos\frac{\pi}{T}(t-nT)-\frac{\pi}{T}\sin\frac{\pi}{T}(t-nT)}{\left(\frac{\pi}{T}(t-nT)\right)^2}$$

$$\frac{d}{dt}Sa\left(\frac{\pi}{T}(t-nT)\right)\Big|_{\substack{t=0\\ n\neq 0}} = \frac{\left(\frac{\pi}{T}\right)^2(-nT)\cos\frac{\pi}{T}(-nT)-\frac{\pi}{T}\sin\frac{\pi}{T}(-nT)}{\left(\frac{\pi}{T}(-nT)\right)^2}$$

$$= \frac{-\cos(n\pi)}{nT} = \frac{(-1)^{n+1}}{nT}$$

$$\frac{d}{dt}p(t-nT)\Big|_{\substack{t=0\\ n\neq 0}} = \frac{(-1)^{n+1}}{nT}\frac{g(nT)}{T}$$

$ISI = \Delta\frac{d}{dt}x(t)|_{t=0}$, and the desired sample is $\frac{a_o g(0)}{T}$, $g(0) = 1$

The relative ISI then is given by

$$ISI = \frac{\Delta\frac{d}{dt}x(t)|_{t=0}}{a_o/T} = \frac{\Delta\sum\limits_{\substack{n=-\infty\\ n\neq 0}}^{\infty} a_n\frac{(-1)^{n+1}}{nT}\frac{g(nT)}{T}}{a_o/T}$$

$$= \frac{\Delta}{T}\sum_{\substack{n=-\infty\\ n\neq 0}}^{\infty}(-1)^{n+1}(a_n/a_o)\frac{g(nT)}{n}.$$

A3. The Optimum Rolloff Function for the LMS Design

The fundamental differential equation of Euler states that $\int_{x_o}^{x_1} F(x, y, y')dx$ is minimum if the function $\frac{dF_{y'}}{dx} - F_y$ vanishes identically in x where $F_y = \frac{dF}{dy}$ [14].

This is equivalent to requiring that the function $y(x)$ satisfies the differential equation

$$y''F_{y'y'} + y'F_{y'y} + F_{y'x} - F_y = 0 \qquad \text{(A2-1)}$$

with the conditions that y, y' are continuous and constant at end points x_0, x_1 and y'' is piecewise continuous, in the general case.

In the special case that $F(x, y, y')$ does not depend explicitly on y' the Euler equation (A2-1) reduces to $F_y = 0$ which is the case we have, and the LMS timing error (2-20):

$$E_t = \left(\frac{2\pi}{T}\right)^2\left[\frac{1}{6} - 4T\int_0^{\alpha/2T} B(f)[1-B(f)]df + 8T^2\int_0^{\alpha/2T} fB(f)df\right]$$

is minimum if

$$\int_0^{\alpha/2T} F(f, B)df = \int_0^{\alpha/2T} [2TfB(f) - B(f)[1-B(f)]]df = 0$$

is minimum, which occurs if

$$\frac{d}{dB}F(f, B) = \frac{d}{dB}[2TfB(f) - B(f)[1-B(f)]] = 0$$

i. e, $2Tf - (1-B) - B(-1) = 0$, which results in

$$B(f) = \frac{1}{2} - Tf, \quad 0 \le f \le \alpha/2T \qquad \text{(A2-2)}$$

A4. Linear Phase Polynomials [24]

$$H(s) = \frac{1}{d(s)} = \frac{1}{1 + b_1 s + b_2 s^2 + \ldots + b_n s^n} \tag{A3-1}$$

Expressing $d(s)$ as sum of even and odd parts $d(s) = d_e(s) + d_o(s)$, then

$$-j\tan(\theta) = \frac{d_o(j\omega)}{d_e(j\omega)}, \qquad \theta = \angle H(j\omega) \tag{A3-2}$$

For an ideal filter $\theta = -\omega$ (after suitable scaling)

$$-j\tan(\theta) = j\tan(\omega) = \tanh(j\omega). \tag{A3-3}$$

Let $s = j\omega$, then the transcendental function $\tanh(s)$ must be approximated by the rational function $\frac{d_o(s)}{d_e(s)}$, which has a zero at $s = 0$, so begin by inverting it to remove a pole at the origin, after which the remainder is inverted and so on, the expansion is as follows:

$$\tanh(s) = \cfrac{1}{\frac{1}{s} + \cfrac{1}{\frac{3}{s} + \cfrac{1}{\frac{5}{s} + \cfrac{1}{\frac{7}{s} + \ldots}}}} \tag{A3-4}$$

All coefficients > 0, so $\frac{d_o(s)}{d_e(s)}$ is a reactance function and $d(s)$ is Hurwitz.

The coefficients of the maximally flat delay polynomial $d(s)$ are given in closed form by

$$b_i = \frac{\binom{n}{i}}{\binom{2n}{i}} \frac{2^i}{i!} \qquad \text{(A3-5)}$$

The above can be generated by a recurrence relation as follows:

Let

$$Q_n(s) = d(s)/b_n \ , \quad Q_1(s) = s + 1 \ , \quad Q_2(s) = s^2 + 3s + 3$$

then

$$Q_{n+1}(s) = (2n + 1)Q_n(s) + s^2 Q_{n-1}(s), \quad n = 2, 3, \ldots \qquad \text{(A3-6)}$$